STUDY OF EFFECTS OF MAGNON-EXCITON INTERACTION ON FERROMAGNETISM OF DILUTED MAGNETIC SEMICONDUCTORS

By

Dereje Fufa

A **Thesis** Submitted to

the **Department of Physics** Addis Ababa University

In Partial Fulfillment of the Requirements for the

Degree of Masters of Science in Physics

June 2017

Addis Ababa, Ethiopia

Addis Ababa University

Department of Physics

STUDY OF EFFECTS OF MAGNON-EXCITON INTERACTION ON FERROMAGNETISM OF DILUTED MAGNETIC SEMICONDUCTORS

By

Dereje Fufa

Approved by the Examination Committee

Chairman: Dr. Deribe Hirpo

Examiner: Dr. Teshome Senbeta

Examiner: Dr. Belayneh Mesfin

Advisor: Dr. Chernet Amente

Acknowledgements

From the very beginning, I would like to thank the Almighty God who brought me into this picture. Wishing him a blessing, I would like to truly express my deepest gratefulness to my advisor Dr. Chernet Amente for his non-stopping guidance to a blend of physics, different softwares, assistant and follow up while carrying out the thesis work. I really admire his friendly approach with immeasurable and valuable contribution throughout the whole period of the research work. I would like to thanks the department of physics of AAU for providing all the facilities and financial support during my study and my heart felt gratitude goes to the MOE which give this chance. I have special heart for my brother Negera Fufa who really feels my business and provides me all my requirements. Eventually, thanks be to my friends for all kinds of encouragement and support I get from them.

Dedication

This work is dedicated to:

My Daughter: **Fenet Dereje**

and

My Son: **Nahil Dereje**

Table of Contents

List of Tables

List of Figures

Abstract

In this thesis the effect of exciton-magnon interaction on Diluted Magnetic Semiconductors (DMS) is theoretically studied employing quantum field theory. The double time temperature Green function technique is used to find dispersion whereby single mode magnon number is obtained from spectral density calculations. It is understood that the existence of exciton and magnon coupling increases total number of magnons which is the reason for decrease in magnetization leading to lowering of ferromagnetic transition temperature T_c. This is perhaps due to scattering of orientations of introduced magnetic spins. The disorder is attributed as enhanced by long time coupling of electron-hole pair, reducing number of holes that mediate ferromagnetism. At lower temperatures the impurity concentration, x and T_c direct relation is known to violate due to the $T^{1/2}$ containing factor dominance.

Introduction

Solid state materials can be grouped into three classes: insulaters, semiconductors and conductors [1]. Semiconductor include a large number of substances widely different chemical and physical properties [2]. Semiconductors are solids in which the highest occupied energy band(the valance band) is completely full at $T = 0k$, but in which the gap above this band is also small so that electron may be excited thermally at room temperature from the valance band to the next higher band which is known as conduction band [3].In recent years, a number of compound semiconductors have found applications for various devices. In addition to binary compound semiconductors, ternary compounds are made for special applications [1]. The semiconductor, specially GaAs is mainly used for high-speed Electronics and photonic applications [4]. Semiconductor such as Silcon(Si) and Galium Arsenide (GaAs), do not contain magnetic ions and are non magnetic. Since late 1980s, people have noticed that in many semiconductor crystals, substitution of a transition metal elements for host semiconductors adds local magnetic moments to the system, forming diluted magnetic semiconductors (DMSs) and usually a transition elements substitute a small fraction, x, of a host semiconductor element sites [5]. Conventional electronics are based on the charge of the electron. Attempts to use the other fundamental properties of an electron, its spin, have been rise to a new rapidly evolving field known as spintronics field involved overseeing the development of advanced magnetic memory and sensors based on spin transport electronics [6]. Spin relaxation (how spin are created and disappear) and spin transport (how spin move in metals and semiconductors) are fundamentally important not only as basic physics questions but also because of their demonstrated value as phenomena in electronic technology [7]. Electrical properties

are characterized by electrical conductivity, carrier mobility, voltage profile and electrical current, while spin properties are characterized by magnetization, magnetic resonance frequencies and spin relaxation rate [8].

This thesis is organized in the following way.

Chapter 1 starts with semiconductors and magnetism covered in this thesis. We provide the energy band gap structure in solid which determines whether the solid is an insulator or conductor or semiconductor. Furthermore the compound semiconductors have high performance of optical characteristics, higher power and higher frequency than elemental semiconductors. Depending on the alignment and interaction between atoms within material, microscopic behavior of the system can be very different. The purpose of this chapter is to give a theoretical view of all the terms of semiconductor and magnetism treated in this thesis. In Chapter 2, we explicitly consider diluted magnetic semiconductors formed from transition metals (mainly Mn) doped II-VI, III-V and IV-VI compound semiconductors. We will focus on spintronics materials and devices. DMS materials play important role in developing spintronics devices due to the advantage of simultaneously utilizing the charge and spin of electrons for information process. In Chapter 3, spin waves and excitons are discussed. Spin waves are collective excitations in ordered spin systems. The collective excitations consists in the propagation of spin deviation, θ. A localized spin at a site is said to under go a deviation when its direction deviates from the direction of magnetization of the solid below the critical temperature. Excitons in a material are quasiparticles that can be considered as hydrogenic bound states of an excited electron in the conduction band and remaining hole in the valance band. In Chapter 4, mathematical technique of Green functions applicable to quantum field theory is introduced. Green function is used to describe the average behavior of particles. In Chapter 5, exciton-magnon interaction starting with the model hamiltonian that consists free magnon, free exciton and magnon-exciton interaction energy, the number of magnons and magnetization are studied. In chapter 6, conclusion of the thesis is given.

Chapter 1

Semiconductors and Magnetism

1.1 Semiconductor Theory

Starting with innovation of the transistor by Barden, Brattain and Shockley in 1947 [1] the technology of semiconductors has exploded. Currently, devices like modern desktop or laptop computers would be unthinkable without microelectronic semiconductor devices. The electrical conductivity of semiconductors can be varied in magnitude widely as a function of (i)impurity content (e.g., doping, typically about 10^{-6} to 1 g of impurity atoms in 1 kg of semiconductors), (ii) temperature (i.e., thermal excitation) and (iii) optical excitation (i.e., excitation with photons having energies greater than the energy gap E_g [1, 2]. When donor impurities are added to intrinsic semiconductors, the number of electrons increase, whereas when accepter impurities are added, the number of holes increase [3]. Donors are impurities that are ionized positively by introducing an electron to the conduction band, while accepters are ionized negatively by accepting electrons from valance bad [4]. Such capability of varying (or controlling) the electrical conductivity over order of magnitude in semiconductors gives unique applications of these materials in different electronic devices [2]. The band structure in solid determines whether the solid is an insulator, a conductor or semiconductor, which semiconductor has sufficiently small energy band gap, E_E, which makes it different from metal and insulator. The characteristics of conductor that a conduction band either is partially filled or overlaps with the valance band so that there is no band gap, whereas insulators are characterized by a large band gap on Fig. 1.1 [4]. Semiconductors constitute a large class of substances which have resistivity lying between those of insulators and conductors. The resistivity

Table 1.1: Energy between Valance Band and Conduction Band of Si and Ge.

Element	0 K	300 K	Gap
Silicon (Si)	1.17	1.11	Indirect
Germanium(Ge)	0.44	0.66	Indirect

of semiconductors reduce to a very great extent with an increasing in temperature [1].

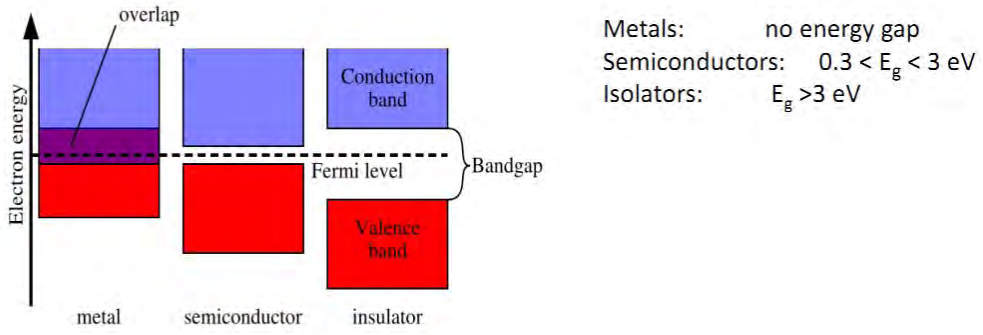

Figure 1.1: Energy band gap for metal, semiconductors and insulator [7].

1.1.1 Types of Semiconductors

1.1.2 Elemental Semiconductors

In Mendeleev's periodic table, the best known class of elemental semiconductors are in the group IV, which are composed of a single species of atoms are silicon(Si) and Germanium(Ge) [1, 5]. Currently, silicon is one of the most studied and used elemental semiconductors and its technology is by far the most advanced among all semiconductors, the main reasons are: (i) silicon devices exhibit better at room temperature (ii) silicon is second only to oxygen in abundances (iii) economic consideration [1].

Intrinsic conductivity and carrier concentration are largely controlled by E_g/k_BT (ratio of band gap to the temperature), where K_B is the Boltzmann's constant and T is the temperature. When the ratio is large, the concentration of carriers and conductivity be low [6]. The intrinsic concentration at a given temperature is higher in Ge than in silicon, because the energy gap is narrower in Germanium (0.66 eV) than in silicon(1.11 eV), as shown in Table 1.1 [6].

1.1.3 Electron and hole statistics of intrinsic semiconductor at equilibrium

Thermal excitation of electron from valance band to conduction band makes the bottom of conduction band populated by electrons and valance band by holes as shown in Fig.1.2 [7].

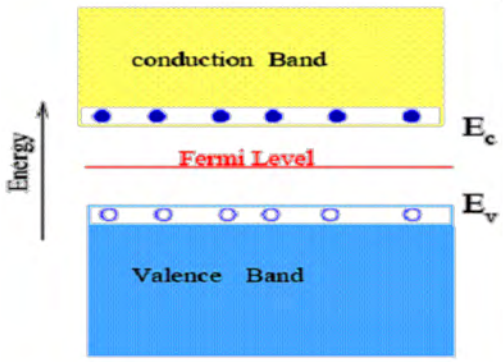

Figure 1.2: Aggregate band diagram for an intrinsic semiconductor [9].

In semiconductor, the mobile electrons are those occupying the energy state E greater than E_c where E_c is the bottom of the conduction band. In the analysis and description of various process in semiconductors, it is essential to calculate the electron concentration in conduction band. The concentration of electron is proportional to (i) the number of states per unit volume and per unit energy (i.e., density of states (DOS) D(E)), over the energy interval between E and E+dE (ii) the probability that energy level E is occupied by electron states in the energy range (E, E+dE) i.e., Fermi-Dirac distribution function $f(E)$ [2] is given by

$$f(E) = \frac{1}{1 + exp\left(\frac{E-E_F}{k_B T}\right)} \tag{1.1.1}$$

To find the concentration of electron in the conduction band, we multiply the density of states with probability that each energy level will have an electron with probability f(E) and integrate across the conduction band.

$$n = \int_{E_c}^{Top\ of CB} f_E(E) D_E(E) dE = \int_{E_c}^{\infty} f_E(E) D_E(E) dE \tag{1.1.2}$$

where E_c is the bottom of the conduction band. $E_c - E_F \geq 4k_BT(4times26\ meV = 104\ meV = 0.1eV)$. For non degenerate semiconductor, the energetic distance between the conduction(E_{CB}) minimum and the fermi level (E_F) should not be much smaller than 0.1 eV at room temperature [7]. For electrons in conduction band $E > E_c$ and $E - E_c \gg k_BT$ shows the probability of a state being occupied decreases exponentially with increasing E in this energy region. Therefore, $e^{\frac{E-E_F}{k_BT}} \gg 1$ (very large number compered with 1). Thus, Eq. (1.1.1) becomes

$$f_{e(E)} \approx e^{\frac{-(E-E_F)}{k_BT}} \tag{1.1.3}$$

The density of state of the conduction band is given by

$$D_E(E) = \frac{1}{2\pi^2}\left(\frac{2m_e}{\hbar^2}\right)^{3/2}(E - E_c)^{1/2} \tag{1.1.4}$$

States near the bottom of the conduction band represent electrons that are nearly free to move from atom to atom with an effective mass m_e^*: the energy of the motion must be calculated from the bottom of conduction band, replacing E with $E - E_c$ and m_e with m_e^* [7]. It is convenient to use $E - E_c$ as a variable to deal with states in the conduction band. De(E) vanishes for $E < E_C$.

By substituting Eq. (1.1.3) and (1.1.40 in Eq. (1.1.2), we obtain

$$n = \int_0^\infty \frac{1}{2\pi^2}\left(\frac{2m_e}{\hbar^2}\right)^{3/2}(E - E_c)^{1/2}e^{\frac{(E_F-E)}{k_BT}}dE \tag{1.1.5}$$

$$n = \frac{1}{2\pi^2}\left(\frac{2m_e^*}{\hbar^2}\right)^{3/2}\int_0^\infty e^{\frac{(E_F-E)}{k_BT}}(E - E_c)^{1/2}dE \tag{1.1.6}$$

Introducing a new variable $x = \frac{E-E_c}{k_BT}$

$$n = \frac{1}{2\pi^2}\left(\frac{2m_e^*}{\hbar^2}\right)^{3/2}\int_0^\infty e^{\frac{(E_F-xkT-E_c)}{k_BT}}(kT)^{3/2}x^{1/2}dx \tag{1.1.7}$$

$$= \frac{1}{2\pi^2}(\frac{2m_e^*kT}{\hbar^2})^{3/2}e^{\frac{(E_F-E_c)}{k_BT}}\int_0^\infty e^{-x}x^{1/2}dx \tag{1.1.8}$$

$\int_0^\infty x^{1/2}e^{-x}dx$ is of a form known as a gammaa function and is equal to $\sqrt{\pi}/2$.

The electron concentration is reduced to the expression

$$n = 2\left(\frac{m_e^*k_BT}{2\pi\hbar^2}\right)^{3/2}e^{\frac{(E_F-E_c)}{k_BT}} \tag{1.1.9}$$

The concentration of electron is still not known explicitly because the Fermi energy is so far unknown.

To evaluate the holes concentration in valance band, the same idea is employed. The probability of an energy state being occupied by holes is the probability of it not being occupied by electron, i,e., $1 - f_e(E)$. That is

$$1 - f_e(E) = 1 - \frac{1}{e^{\frac{(E-E_F)}{k_B T}} + 1} = \frac{1}{e^{\frac{(E_F-E)}{k_B T}} + 1} \tag{1.1.10}$$

For holes in valance band $E < E_v$, this shows $(E_F - E) \gg k_B T$ and $e^{\frac{E_F-E}{k_B T}} \gg 1$. Thus, the distribution function of holes is given by

$$f_h(E) = \frac{1}{e^{\frac{(E-E_F)}{k_B T}} + 1} \approx e^{\frac{-(E_F-E)}{k_B T}} \tag{1.1.11}$$

Density of state for holes is

$$D_h(E) = \frac{1}{2\pi^2}\left(\frac{2m_h^*}{\hbar^2}\right)^{3/2}(E_v - E)^{1/2} \tag{1.1.12}$$

The hole concentration in conduction band is given by

$$p = \int_{bottom\ of\ VB}^{E_V} D_h(E) f_h(E) dE \tag{1.1.13}$$

where E_v is energy of the valance band edge.

$$p = \frac{1}{2\pi^2}\left(\frac{2m_h^*}{\hbar^2}\right)^{3/2} \int_{-\infty}^{Ev} (E_v - E)^{1/2} e^{\frac{-(E_F-E)}{k_B T}} dE \tag{1.1.14}$$

In the same way we did for electron, the concentration of holes in valance band is

$$p = 2\left(\frac{m_h^* k_B T}{2\pi\hbar^2}\right)^{3/2} e^{\frac{E_v - E_F}{k_B T}} \tag{1.1.15}$$

It is well known that the number of electrons in the conduction band equals the number of holes in the valance band in intrinsic semiconductors. This is due to the fact that, electrons make transition to the conduction band leaving holes behind. However, doping would change the situation, as can be learned from Eq. (1.1.15). In our case magnetic impurities are introduced as acceptors adding extra holes that are thought as enhancing magnetization and hence the Fermi level is supposed to shift towards the top of the valence band.

1.1.4 Compound Semiconductors

Binary compound semiconductors can be synthesized by combing elements from column II and VI (ZnTe, ZnSe, ZnS, CdSe, CdTe and CdS), III and V (GaAs, GaN, InP, AlSb, GaP, AlP, and AlAs) and IV-VI the lead chalcogenides that are PbS, PbSe and PbTe [4, 2]. Most binary compound semiconductors are direct band gap (E_{CB} minimum and E_{VB} maximum at the same K value) materials. In Fig. (1.3), AlAs and GaP are two of the few compound semiconductors with indirect energy band gap (E_{CB} minimum and E_{VB} maximum at the different K value [10]. Compound semiconductors which have direct energy gaps, efficient emission or absorption of electromagnetic radiation can be expected in these materials [11, 8]. They have high absorption coefficient that sun light is absorbed with in a small range beneath the surface possibility to fabricate thin film solar cells [7]. Compound semiconductors with direct energy band gap and narrow energy gap that have energy gap below about 0.5 eV, large photocurrents are favored by these materials, because semiconductors only absorb photons with energies greater than the band gap. Therefore, narrow gap materials absorb large fraction of the solar spectrum and they are extensively employed in such inferared optoelectronics device application as detectors, specially (PbS) and (PbSe) detectors can be employed in special range of wavelength between 1 and 6 μm [2]. Wide energy band gap compound semiconductors have high melting point. The wide energy gap of II-VI compounds and some III-V compounds, such as GaN and AlN ensures that various electronic devices can operate at relatively high temperature(greater than 600^0C) [2]. Compound semiconductors offer high performance of optical characteristics, higher frequency, higher power than elemental semiconductors and greater device design flexibility due to mixing of materials [9]. Compound semiconductors also allow to perform band gap engineering by changing the energy band gap as a function of position that allows the electrons to see engineered potential which guide electrons or holes in specific direction or trap them in specific regions of devices designed by electrical engineer [12]. The effect of accepter and donor impurities and defect in compound semiconductors are significantly different from those elemental semiconductors [2].

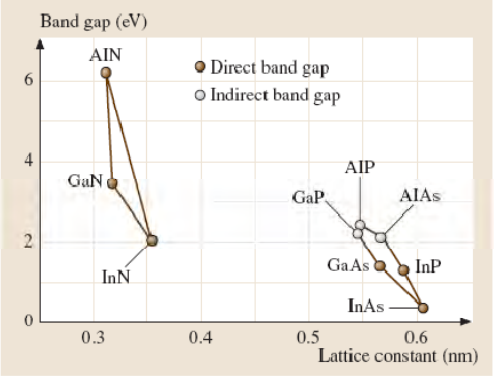

Figure 1.3: Room temperature energy band gap for important III-V materials versus their lattice constant for both direct and indirect-gap semiconductors [2].

1.2 Magnetism

Magnetism cannot be separated from electricity, because electron revolving around a nucleus in an atom produces a small magnetic field. In atoms of most materials the electrons orbits are more or less random. Because of this reason the magnetic fields generated by individual electrons gets canceled. Also spins are paired and therefore, their magnetic effects cancel each other. Further the thermal agitation in materials does not permit any possible alignment of magnetic moments. Therefore, most materials do not have any magnate in the absence of magnetic field [13]. Therefore, we use the term magnetism to describe how the atoms of materials respond to a magnetic field.

1.2.1 Source of Magnetism

Magnetism in material arises from the fundamental property of an electron such as intrinsic spin magnetic dipole moment due to rotation of an electron on its axis and orbital magnetic dipole moment due to revolution of an electron about its nucleus produce a small magnetic field like current flowing through a coil produces magnetic field [13]. Therefore, each electron in an atom has two magnetic dipole moments associated with it. One is for its spin and the other is for its orbit. For most materials these two dipole moments can combine vectorially for each electron and the resultant vector for the whole atoms

often canceling each other. For some materials each atom has a non zero dipole moment, but because of the atom have all different orientations the material as the whole remains non-magnetic.

The Bohr magneton μ_B is defined as the magnetic moment originated from spin motion of a single electron which is the smallest unit of magnetic moment of solid [14, 15].

$$\begin{aligned} \mu_B &= \frac{e\hbar}{2m_0} \\ &= 9.27 \times 10^{-24} Am^2 \end{aligned} \tag{1.2.1}$$

where $\hbar$ is plank's constant, e is charge on electron and m_0 is mass of electron. The collective behaviors of all atoms within the system determine the magnetic behavior [16]. Depend on the alignment of and interaction between atoms within a material, the observed microscopic behavior of the system can be very different [17]. The fundamental types of magnetism in a material system are described below:

1.2.2 Diamagnetism

In diamagnetic materials the atoms have no net magnetic moment and internal magnetic moment interaction when there is no applied magnetic field. Under an applied magnetic field, electrons in an atom orbital will slightly adjust their orbit in such a way to create current loops which induce small magnetic moment that oppose the applied field [16]. This is materials analogy of Lenz's law, where a changing magnetic field induces a current in a coil of wire opposite the direction of applied field [1]. Fig. 1.4 showsthe magnetic moments add up to gather gives up internal magnetization in opposite direction to applied magnetic field, but magnetization vanished immediately when applied field is removed. Diamagnetic materials have weak negative susceptibility ($\chi_m < 0$) and can be observed only in atoms with complete electron shell result no magnetic moment [18]. Diamagnetism is roughly independent of temperature, only in the case of superconductors with a resistivity is equal to zero at low temperature, will have their mobile charges responding without resistance to the external field and the induced magnetic moments will exactly cancel external magnetic field and magnetic field cannot penetrate the superconductor materials [19]. Using Langevin theory, the magnetic susceptibility of a diamagnetic material is given by

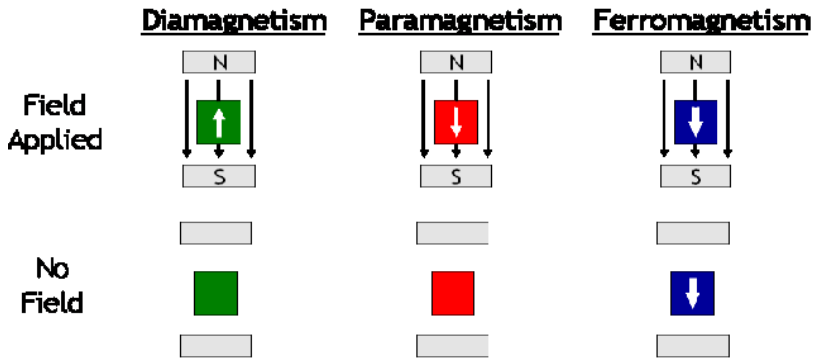

Figure 1.4: Macroscopic behavior observed in diamagnetic, paramagnetic and ferromagnetic materials. In diamagnetic materials, the internal magnetization aligns antiparallel as the material 'rejects' the applied magnetic field. In paramagnetic materials, the internal magnetization aligns weakly with the applied field, but vanished after the magnetic field is removed. In ferromagnetic materials, the magnetization aligns strongly with the applied magnetic field and maintains this alignment after the field is removed [20].

the expression

$$\chi_{Dia} = -\frac{\mu_0 N Z e^2 < r^2 >}{6m} \tag{1.2.2}$$

here N is number of dipoles per unit volume, e is charge on an electron, m is mass of electron $< r^2 >$, is the average of square of atomic radius r, z is atomic number and μ_0 is the pearmebility of free space.

1.2.3 Paramagnetism

An other configuration of spins in materials whose atoms unpaired spins is known as paramagnetism. In this case, in steady of having a collective alignment of spins on the individual atoms, Fig. 1.5, the atoms are aligned in random direction: here the material has no over all magnetic moment, since all the spins cancel each other. This happens in ferromagnetic materials above Curie temperature, where the thermal energy of the system is able to overcome the exchange energy and material loses its magnetic ordering [21]. The over all behavior in the presence of magnetic field is very similar to that of a diamagnetic materials, with the exception that the magnetic susceptibility (χ) is positive rather than negative. In Fig.1.4, as field is applied, there is a tendency of spins to align with the magnetic field. When the field is removed, the atoms resume their random alignment and

there is no net magnetic moment.

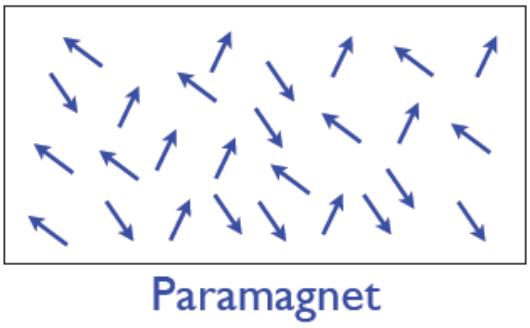

Figure 1.5: Schematic showing the magnetic dipole moments randomly aligned in paramagnetic sample [6].

Magnetic susceptibility of paramagnetic material varies with temperature according to the Curie law.

$$\chi_p = \frac{C}{T} \tag{1.2.3}$$

where, C is Curie constant. It predicts the inverse relationship between paramagnetic susceptibility and temperature with $\chi_p = 0$, as $T \longrightarrow \infty$ Fig. 1.6.

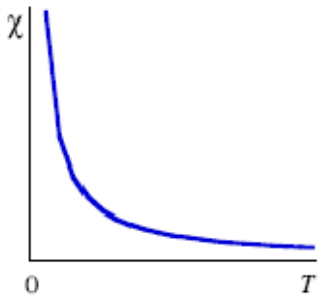

Figure 1.6: Temperature dependence of the magnetic susceptibility of paramagnetism [22].

1.2.4 Ferromagnetism

In ferromagnetic materials, there are important interactions between magnetic moments that energetically favorable magnetic alignment of spin will be in parallel direction in the absence of magnetic field as showen in the Fig. 1.7, leading to spontaneous magnetization [22]. The huge difference between a ferromagnetic and diamagnetic is the degree of alignment achieved, but not to any large differ in the size of moment per atom. The best known examples of ferromagnetic materials are the transition metals Fe, Co and Ni which have unfilled 3d energy levels and rare-earth elements related to unfilled 4f energy levels. However, all elements possessing incomplete energy levels are not ferromagnetic [16]. In Fig. 1.4, the internal magnetization is directed in the same direction with applied magnetic field and maintain this alignment after the field is removed [20].

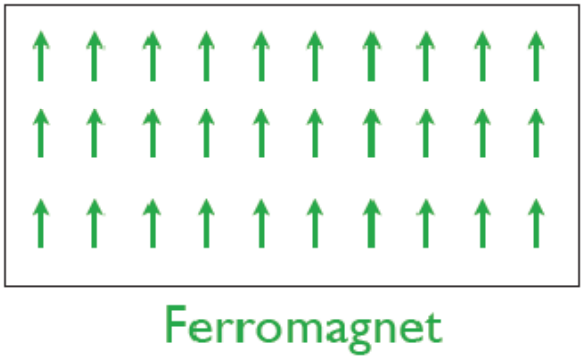

Figure 1.7: Magnetic ordering of Ferromagnetic.

1.2.5 Antiferromagnetism and Ferrimagnetism

Fig. 1.8 (a) illustrates an antiferromagnetic arrangement, in which equal spins but, adjacent moments pointing in opposite directions. Thus the moments balance each other, resulting in a zero net magnetization [23]. Another type of arrangement is the ferrimagnetic pattern shown in the Fig. 1.8 (b), neighboring magnetic moments are in opposite direction, but since in this case the moments are unequal, they do not balance each other complectly and there is net magnetization.

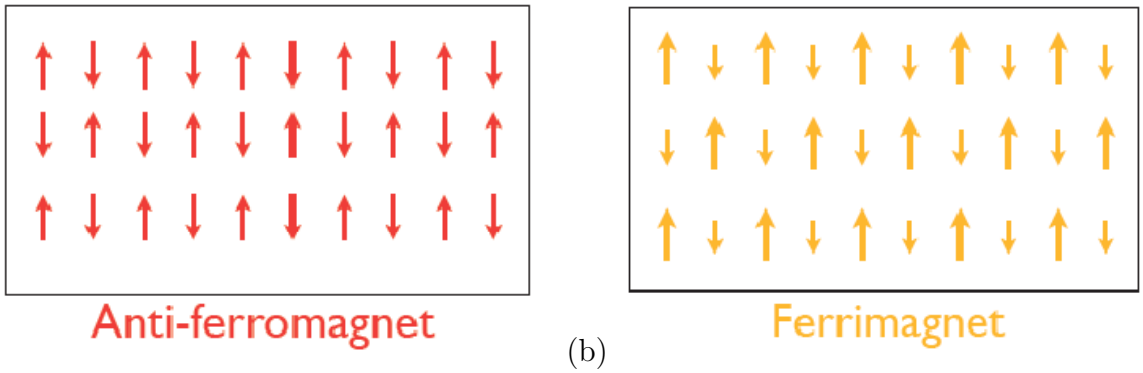

(a) (b)

Figure 1.8: (a) Magnetic order of Antiferromagnetism (b) Magnetic order of Ferrimagnetism materials.

1.2.6 Ferromagnetic Transition Temperature

Ferromagnetism refers to solids that are magnetized without applied magnetic field, and these materials are said to be spontaneously magnetized [24]. Above Curie temperature T_c as shown in Fig. 1.10 all ferromagnetic materials become paramagnetic, because of the thermal energy is large enough to overcome the cooperative ordering of the magnetic moments [21]. Curie temperature (T_c) is the temperature at which this transition occur. When temperature rise beyond the curie temperature, there is no longer maintain spontaneous magnetization, it still responds paramagnetically to an external magnetic field [24]. The curie temperature T_c itself is a critical point where the magnetic susceptibility theoretically infinite Fig.1.9 and there is no net magnetization, spins correlation fluctuate at all length scale [22]. In other way, as the temperature increases further, the magnetic ordering and susceptibility decreases. In ferromagnetic materials the spins are magnetized spontaneously, which implies the presence of internal field or molecular field result from all molecules in the sample due to the consequence of Pauli Exclusion principle and the Coulomb interaction between electrons [15]. The effective internal field will linear scale with magnetization M [6]is given by

$$H^{Mol} = \lambda M \tag{1.2.4}$$

where λ is molecular field constant independent of temperature that parameterize the strength of molecular field. The interaction between nearest neighbor atoms of electron

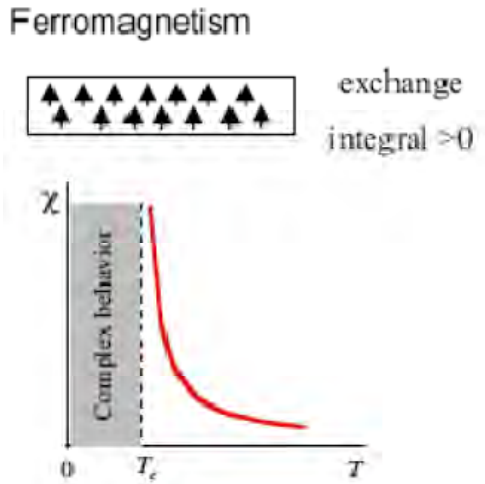

$$\chi_m(T \gg T_c) = \frac{C}{T - T_c}$$

Figure 1.9: Temperature dependence of the magnetic susceptibility of ferromagnet.

of magnetic moments which responsible for producing the molecular field which make adjacent atomic moments parallel to one an other in materials is very similar to that of an applied external magnetic field (leading to alignment) [20]. By considering paramagnetic phase with applied magnetic field H, which causes magnetization and molecular field inside the sample, we shall have ferromagnet, this leads to the effective field [25].

$$H_{eff} = H + H^{Mol} \tag{1.2.5}$$

The susceptibility of material, χ, indicates quantitatively determination of the responses of material to applied magnetic field, and it is defined as the ratio of the magnetization, M, and the applied magnetic field, H. That is

$$\chi = \frac{M}{H} \tag{1.2.6}$$

If χ_p is the paramagnetic susceptibility, the induced magnetization is given by

$$\chi_p = \frac{M}{H^{eff}} = \frac{M}{H + \lambda M} \tag{1.2.7}$$

It can be solved explicitly for the magnitude of magnetization so that

$$M(1 - \chi_p \lambda) = \chi_p H \tag{1.2.8}$$

$$M = \frac{\chi_p H}{1 - \chi_p \lambda} \tag{1.2.9}$$

By substituting Eq. (1.2.11) into Eq. (1.2.9), we find for the susceptibility of the ferromagnetic material

$$\chi = \frac{C}{T - \lambda C} = \frac{C}{T - T_c} \tag{1.2.10}$$

which is the Curie Weiss law. The curie law describes Eq. (1.2.3)the magnetic behavior of ideal paramagnetic materials very well, however, it cannot accurately describe a system when intermolecular interactions are involved. A simple modification to the curie law, based on molecular field theory is the Curie-Weiss law. The curie temperature $T_c = \lambda C$ is the temperature above which the spontaneous magnetization vanishes and it separates the disorder paramagnetic phase $T > T_c$ from the ordered ferromagnetic phase at $T < T_c$ [20] as shown in the Fig. 1.10.

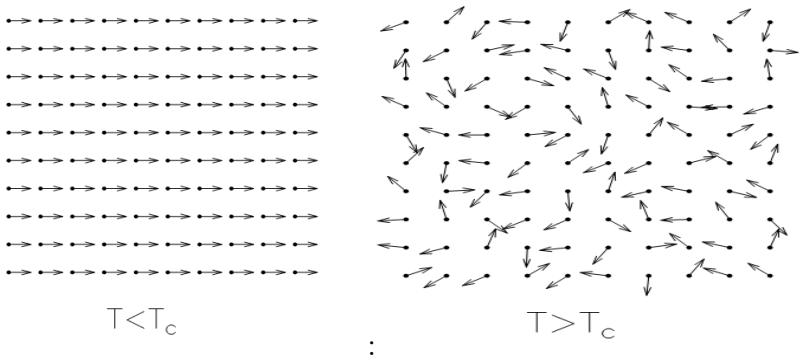

Figure 1.10: Left panel, ferromagnet ($T < T_c$); Right panel, paramagnet ($T > T_c$) phase transition [20].

1.2.7 Antiferromagnetism Transition Temperature

In antiferromagnetic materials, the spin of unpaired electrons align in antiparallel fashion in the absence of an external magnetic field and below a certain critical temperature called Neel temperature T_N [26]. Neel temperature is the temperature at which antiferromagnetic material becomes paramagnetic because of the the thermal energy become large enough to disorder the magnetic ordering in the material [23]. Under relatively

low magnetic field saturation when the the majority of atomic dipoles are not aligned with the field, paramagnetic materials exhibit magnetization according to the well known Curie-Weiss law, which treats the interaction between spins and molecular field. Antiferromagnets are also characterized by a negative value of the curie temperature (T_c) [22] and Eq. (1.2.11) is obtained by replacing T_c in Eq. (1.2.10) by θ_p.

$$\chi_m = \frac{C}{T - \theta_p} \tag{1.2.11}$$

where, θ_p is the Curie-Weiss constant that is indicative of the strength of the intermolecular interactions between spins. In Fig. 1.11, the susceptibility of antiferromagnetism is not infinite at $T = T_N$ but attain maximum at its T_N where there is a well defined kink in the curve χ versus T [22]. The antiferromagnetism susceptibility begins decreasing at Neel temperature. As the temperature decreases further, the magnetic ordering increases and the susceptibility decreases [23].

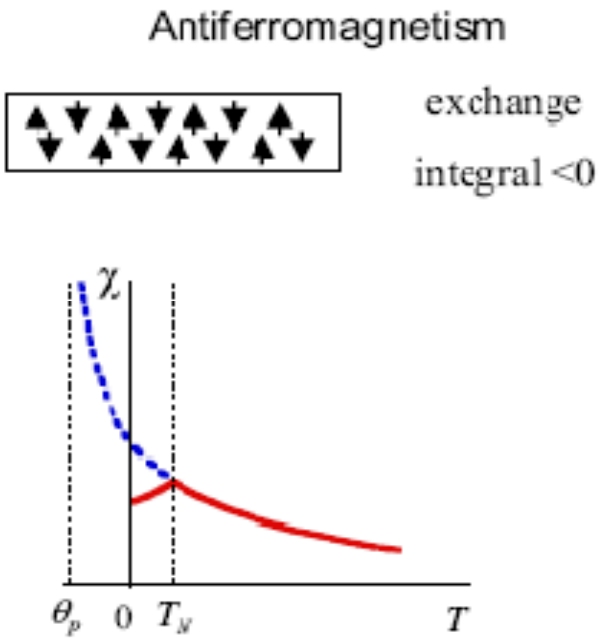

$$\chi_m(T >> T_N) = \frac{C}{T - \theta_p}$$

Figure 1.11: Temperature dependence of the magnetic susceptibility of antiferromagnet [25].

Chapter 2

Overview Of Diluted Magnetic Semiconductors

The potential for a material to posses both magnetic and semiconductor properties has been known and studied since 1960s [27]. One strategy for creating systems that are simultaneously semiconducting and magnetic, initiated in the 1970s is to introduce local moments in well understood semiconductors and the result is a new class of materials now known as diluted magnetic semiconductors (DMSs) [18]. In both semiconductors and magnetic cases, sophisticated and economically important technologies have been developed to exploit the unique electronic properties, initially for information processing in the case of semiconductors and for information storage and retrieval in the case of magnetism [14]. The benefit of diluted magnetic semiconductors based device include reduce power requirements compared to traditional semiconductor devices [15]. This energy gain is due to the reduced power needed to flip an electron spin, as opposite to moving charge in electric field [27]. Technologically, DMSs raise the exciting potential of spintronics applications (logic and memory operators) that in principle seamlessly integrated on a single device [28]. The major obstacle for applications of these diluted magnetic semiconductors (DMS) system is that the curie temperatures are well below room temperature [26, 28]. One major incentive for finding a DMSs materials that can operate at meaningful temperatures is that one could then integrate the new technology with the existing semiconductor industry [14]. T. Diel calculated the curie temperature of different p-type semiconductors doped with Mn ions [24]. He found that it is proportional to the concentration of the impurities and to the square root of the p-type charge carrier concentration.

Recently, the curie temperature of $Ga_{1-x}Mn_xAs$ is found to be increased up to 173 K by means of increasing its crystal quality and the number of Mn impurities up to $x = 0.08$ [28]. In DMSs, low concentration of magnetic impurities carrying localized magnetic moments (spins) form diluted spin system [29]. The field DMS is developing in remarkable fast paste and now a days researchers mainly focus on fundamental aspect, however with deeper and deeper understanding through theoretical and experimental studies when the collaboration between fundamental and applied research on DMS will be increasingly intense and widespread [25]

2.1 Mechanism of Making Non magnetic Semiconductor Magnetic

The usefulness of semiconductors resides in the ability to dope them with impurities to change their properties usually to p-type and n-type. This approach can be followed to introduce magnetic elements into non-magnetic to make them magnetic. This category of semiconductors are called diluted magnetic semiconductors which are alloys of non-magnetic semiconductors as shown Fig. 2.1C. So, Substitution of Ga by transition metal Mn involves the removal of a Ga atom and introduction of a Mn atom at that vacated by Ga. Dilute magnetic semiconductors are a class of magnetic semiconductors [30] and are semiconducting alloys, formed when non-magnetic semiconductor crystal lattice, Fig. 2.1B are replaced substitutionally by magnetic ions of transition metals [31]. Of the total host atoms N, N_{imp} amount of Mn is replacing so that, only $x_m = \frac{N_{imp}}{N}$ percentage is involved in magnetization, therefore, $x_m = \frac{N_{imp}}{N}$ has spin S and x_mS is the total spin where x_m is impurity concentration. In generally, of transition metal atoms (TM), with typically concentration of (3-8) percent are randomly distributed on the cation site [32]. Recent experiments find that Mn atoms occupy both substitutional as well as interstitial positions in GaAs. The discussion of physics that underlies room temperature ferromagnetism interaction metal doped semiconductors has largely focused on substitutional. Interstitial is a position not normally occupied by an atom [6]. At low temperature regime, around 250^0C, there is insufficient thermal energy for surface segregation to occur but is still sufficient for good quality single crystal to form. In addition to the substitution

incorporation of manganese, low temperature molecular beam epitaxy (MBE) also causes the inclusion of other impurities. The two other common impurities are interstitial manganese where manganese atom occupy a site with coordinated by four As atoms and four Ga atoms and arsenic anti-sites where large arsenic atoms occupy gallium sites which act as donor. Both impurities act as double donors, removing the holes provided by the substitutional manganese. The interstitial manganese also bound antiferromagnetically to substitutional manganese, removing the magnetic moment. In generally, Mn interstitial and anti-site defects are both believed to decrease T_c by acting as donors compensating the holes provided by substitutional Mn atoms, which induce ferromagnetism.

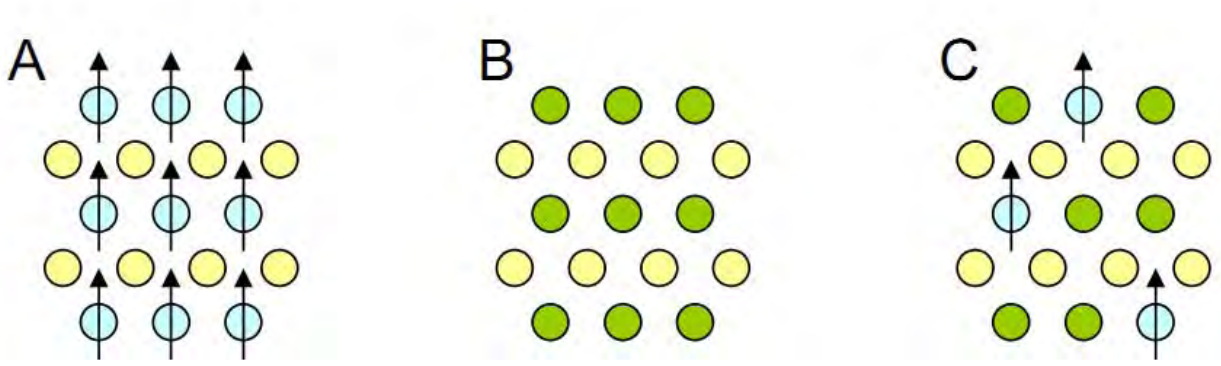

Figure 2.1: Schematic showing (A) a magnetic semiconductor, (B) a non magnetic semiconductor material and (C) a diluted magnetic semiconductor [33].

2.1.1 The Magnetic Elements for Doping

The magnetic elements for doping purpose are mainly Cr, Mn and Fe from transition elements in forming diluted magnetic semiconductors [32]. The Table 2.1 shown below gives the configuration why Mn^{+2} is more appropriate. In Mn^{+2} doped III-V based DMS, there is a valance mismatch between that of Mn and the group III elements with $S = 5/2$ creating holes in valance band. In Cr^{2+} doped III-V, the 3d electrons are less in number $4(1/2) = 2$ less magnetic impurity spins per atom result weak ordering in the compound. In Fe^{2+} the 3d electrons gives rise to S= $4(1/2)= 2$ and Fe^{3+} gives the valance match group III elements as Cr^{2+} in III-V DMS. Therefore, Mn^{+2} is more preferable for doping purpose in introducing high density of magnetic moments and holes to the system [33].

Table 2.1: Magnetic elements used for doping purpose in DMS.

Element	Cr^{24}	Mn^{25}	Fe^{26}	Cr^{+2}	Mn^{+2}	Fe^{+2}	Fe^{+3}
Configuration	$3d^5 4s^1$	$3d^5 4s^2$	$d^6 4s^2$	$3d^4$	$3d^5$	$3d^6$	$3d^5$

2.2 Family of Diluted Magnetic Semiconductors

Europium chalcoginides (EuSe and EuO) and Cr-spinel structured composite for example ($ZnCr_2Se_4$) as the 1960s are studied as magnetic semiconductors [34]. However, the crystals are very hard to be produced in experiment, their low curie temperature T_c (50K or lower), strong insulation and poor semiconducting transport property [29]. Later on, studies have been speeded up on diluted magnetic semiconductors including transition metals (mainly Mn) doped II-VI, III-V and IV-VI compound semiconductors [32].

2.2.1 II-VI based Diluted Magnetic semiconductors

The first DMS to be identified and studied in 1980's were II-VI based DMS obtained by doping Mn^{2+} in to non magnetic semiconductors, ZnSe, ZnS, CdTe, HgSe...etc. The DMS compounds formed are expressed as $(II_{1-x}Mn_x)$VI which are $(Zn_{1-x}Mn_x)Se$, $(Cd_{1-x}Mn_x)Te$, $(Hg_{1-x}Mn_x)Se$, $(Cd_{1-x}Mn_x)S$ and so on. Where x_m is the fraction of magnetic transition metal atoms typically Mn that substitute the group II elements. The magnetic structure in the diluted magnetic semiconductors $Zn_{1-x}Mn_xTe$ and $Cd_{1-x}Mn_xTe$ with $0 \leq x_m < 1$ are interesting one because, several phases may appear including paramagnetic (PM) in $0 \leq x_m \leq 0.2$ for all value of critical temperature, anti ferromagnetic (AFM) $0.6 < x_m \leq 1$ and spin glass (SG) phase $x_m < 0.6$ which are attributed to the randomness and frustration of the antiferromagnetic interaction between the Mn magnetic ions [35]. The problem with controlling the n-type and p-type doping in to these materials, as well as low curie temperature typically below $2k$, served as impediments on the development of II-VI DMS. Nevertheless, this was a precedent to research in to III-V materials as potential DMS candidates [30].

2.2.2 III-V Based Diluted Magnetic semiconductors

III-V based diluted magnetic semiconductors have bean prepared when transition magnetic elements mainly Mn^{2+} (S= 5/2) which mismatch in valance electron with group

Table 2.2: Some III-V based diluted magnetic semiconductors with their curie temperature and concentration of Mn [30, 35].

Group	Materials	$T_c(K)$	X_m
$III-V$	$Ga_{1-x}Mn_xAs$	110 (T_c)	0.05
	$Ga_{1-x}Mn_xN$	940 (T_c)	0.03-0.05
	$Ga_{1-x}Mn_xP$	270 (T_c)	0.03
	$Ga_{1-x}Mn_xSb$	25 (T_c)	0.016
	$In_{1-x}Mn_xAs$	60 (T_c)	0.43
	$Ga_{1-x}Fe_xN$	250(T_c)	0.03-0.05

III elements in doping with III-V semiconductor compounds [33, 30]. In Fig.2.2, when

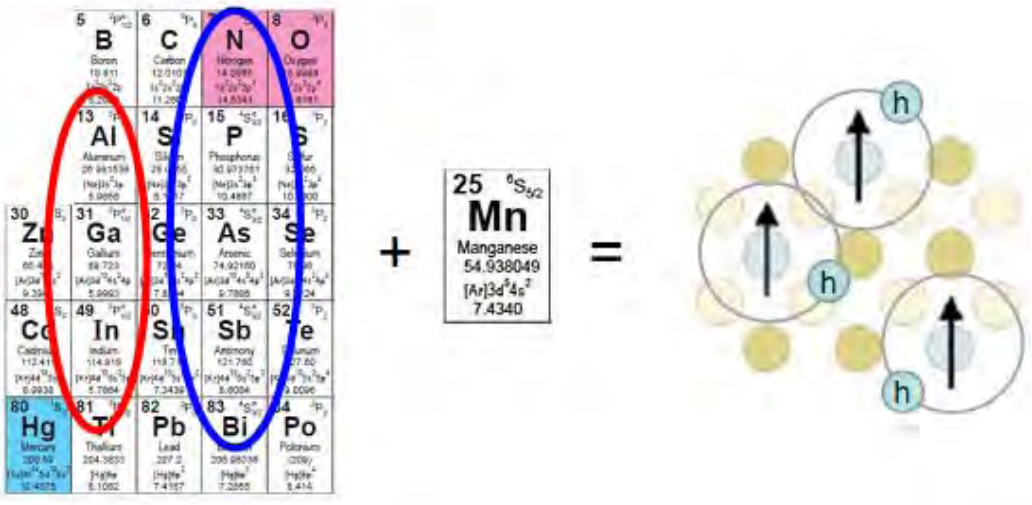

Figure 2.2: Formation of (III,Mn)V diluted magnetic semiconductors [31].

magnetic ion Mn^{++} doped into semiconductor to form DMS, it acts as electron accepter(providing holes) as well as producing magnetic moments. Spin from magnetic ions can capture carriers into its ferromagnetic spin cluster, due to spin-spin exchanging coupling between carriers (interaction between s electrons in conduction band, p electrons in valance band and d electrons from magnetic ions (sp-d exchange interaction)) and interaction between d electrons from magnetic ions (d-d), percolation network is formed in which cluster of the hole are delocalized and hop from site to site, which is an effective mechanism for aligning Mn moments with cluster network [36]. The holes are thought to mediate ferromagnetic coupling between Mn^{2+} ions [30]. The initial work by Ohno

and Munekata on Mn doped InAs opened up the technologically of significant III-V semiconductors as potential hosts for diluted magnetic semiconductors [30]. Among DMS (Ga,Mn)As is the most studied since GaAs is the most useful semiconductor especially in producing optical devices due to its good optical properties and applications in which high speed is required [37]. Therefore, the introduction of magnetic semiconductor based on GaAs opens up the magnetic phenomena, data processing and storage facilities that not present in conventional non-magnetic semiconductor GaAs material in optical and electrical devices already established [38]. Through study of its magnetic transportation, for given Mn concentration x_m, it was found that the curie temperature T_c was always in the range of $2000x_m \pm 10K$ [39]. Later discovered that the curie temperature of (Ga,Mn)As reached its highest 110 k when x_m= 0.05 [34]. When Mn concentration was reduced, curie temperature T_c would also decrease, when Mn concentration x_m, went below 0.005, ferromagnetic would disappear. Moreover, as Mn concentration in (Ga,Mn)As increases, the transportation properties experienced series of changes [39]. The transport measurements show insulating behavior at the lower Mn fraction and metallic behavior at the higher Mn fraction [29]. In insulating case, they found that a relatively small fraction of Mn ions strongly couple to valance band holes. H. Ohno et al., believes that it is hole charges that would lead to ferromagnetism in (Ga, Mn)As and also discovered that the number of Mn ions in (Ga,Mn)As is of the same order compared to those of holes charges [33]. When annealing temperature exceeds 260^0C,the resistivity starts to increase again and the decreasing of T_c follows, and also 260^0C is the critical temperature at which very low MnAs precipitation starts and at 280^0C sign of the precipitation of MnAs resulting in decreasing of the Mn concentration in the (Ga,Mn)As phase of the composite system. However, still there is no clear understanding of the reason for ferromagnetism in Ga, Mn)As [30]. Based on the study of (Ga,Mn)As, other DMS materials with even higher curie temperature T_C has been discovered, for example (Ga, Mn)N [40]. However, it is all not as good in terms of experimental and compatibility with current semiconductors industry. Till now, (Ga,Mn)As is the most promising DMS material in practice [34]. At present time, the critical temperatures are still far below the room temperature and prevent their direct application [35]. As in Fig. 2.3, the curie temperature of Mn doped GaN is the highest ($T_c = 940K$) among various semiconductor compounds [34, 38]

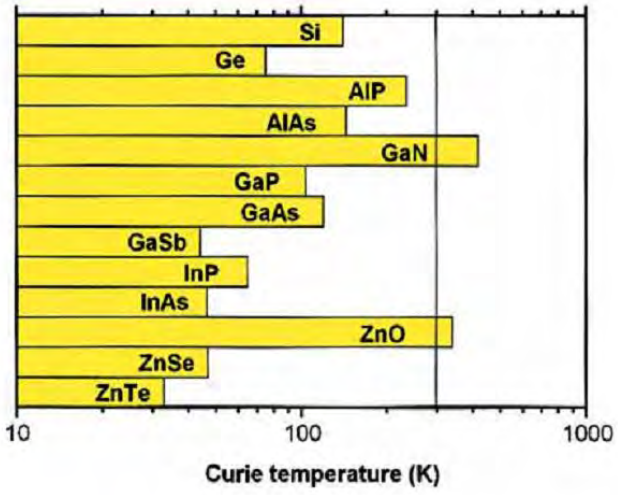

Figure 2.3: curie temperatures of various DMS candidates [30] .

2.2.3 Oxide Diluted Magnetic Semiconductors

When non magnetic semiconducting oxides doping doping by magnetic ions they form the family of diluted magnetic oxides. Various oxides in thin layers seem to exhibite a ferromagnetic behavior at high temperature [23]. Most of the oxide based DMSs are wide band gap semiconductors ($> 3eV$) which can add an optoelectronic dimension to the new generation of spintronics devices. In this context, the ground breaking was the discovery of room temperature ferromagnetism in the $Co : TiO_2$ system by Matsumoto et al. which has triggered a considerable number of investigations in other oxide-based DMS such as transition metals (Mn, Fe, Co and Ni) doped Zno, SnO_2, CU_2O and $In_{1.8}Sn_{0.2}O_3$ [44]. Table 2.4. Seong et al. showed that at Co contents $x_m \leq 0.05$ Co doped TiO_2 thin film display an homogeneous structure with out any clusters and exhibit pure ferromagnetic properties that can be attributed to the $Ti_{1-X}Co_xO_2$ phase, the left figure in Fig.2.4. In contrast as shown the right figure in Fig.2.4, at $x_m > 0.05$ clusters having soft magnetic (SM) properties are formed in the homogeneous $Ti_{1-X}Co_xO_2$ matrix and over all magnetic behavior that depends on the ferromagnetic properties of both $Ti_{1-X}Co_xO_2$ and Co cluster [41]. In 2001 Matsumoto represented that $Co : TiO_2$ (doped Co below 5 percentage) film made at room temperature ferromagnetism and its cure temperature $T_c > 400K$ [28]. currently there is no consensus on the origin of ferromagnetism in Co

Table 2.3: Some reports on high T_c oxide-based DMS [30].

Materials	Doping(x)in percentage	Moment(μ_B)	$T_c(K)$	$Eg(ev)$
TiO_2	Co, 1-2	0.3	> 300	
	Co, 7	1.4	650-700	3.2
	Fe, 2	2.4	> 300	
ZnO	Co, 10	2	280-300	
	Mn, 2.2	0.16	> 300	3.3
	Fe , 5	0.75	> 550	
	Ni, 0.9	0.06	> 300	
SnO_2	Co, 5	7.5	650	3.5
	Fe,5	1.8	610	
Cu_2O	Co, 5	0.2	> 300	
$In_{1.8}Sn_{0.2}O_3$	Mn, 5	0.8	> 300	

doped TiO_2, in particularly, whether it is extrinsic effect due to direct interaction between the local moments in spin of the carriers and the local magnetic moments. Mn doped SnO_2 is predicated as an other oxide DMS. H. Kimura discovered magnetoresistance in Mn doped SnO_2 at low temperature 5 K [42]. Numerous reports of the magnetic properties of transition metal doped ZnO (sample $Zn_{1-x}Mn_xO$) have appeared recently. Ueda, et al reported cuire temperature above $300K$ for Co doped ZnO, Jung et al. at T_c of $45K$ for Mn doped ZnO and Wakano. et al. at T_c of $2K$ Ni doped ZnO. For the film doped with 3-25 percentage Ni ferromagnetic was observed at $2K$, above $30K$ Superparamagnetic behavior was observed [40]. In general, with an initial influx interest, the novel materials such as GaAs doped by Mn, GaN doped by Mn, ZnO doped by Ni and Mn and InP doped by Mn have been fabricated, but in order for these materials to be of use in spintronics devices, room temperature is a necessity [39]. Theoretical predictions made by Diet et al.have indicated that both GaN as well as ZnO have the potential to be ferromagnetic at room temperature [43].

2.3 Spintronics Materials and Devices

2.3.1 Fundamental concept of spintronics

Spintronics is a branch of electronics emerged from the diluted magnetic semiconductors in aspect of utilization of the spin in addition to the charge of the carrier in semiconductor [41]. The importance of the spin of electrons was first realized after the discovery of the

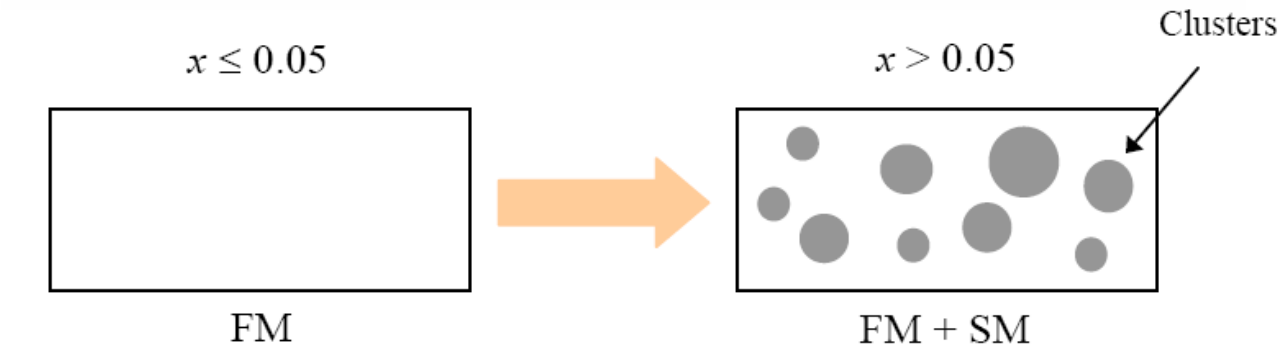

Figure 2.4: The right figure demonstrates microstructural model representing the influence of Co content on magnetic properties of $Co_xTi_{1-x}O_2$ thin film and absence of Co cluster is shown in the left one.

GaintMagneto Resistance (GMR) in 1988, which result high density data storage devices, MRAM [38]. There are two main categories of spintronic devices, passive and active. Passive spintronics devices make use of spin degrees of freedom, like magnetic RAM and magnetic read heads the net polarization of spins in a material is used for data storage and retrieval; active manipulation is not necessary [42], whereas in active spintronics devices which employ both the spin and charge degrees of freedom, rely on manipulation to generate versatile devices with the capability of both traditional electronics and passive spintronics [44]. Spin is an intrinsic quantum property of electrons and is closely related to magnetism [40]. In the simplest model, an electron can be depicted as a charged spinning ball which has mass, charge and is either "spin up" and "spin down" states [36]. In many materials, electron spins are equally present in both the up and the down state and no transport properties are dependent on spin, therefore, spintronics devices requires generation or manipulation of spin polarized population of electrons, resulting an excess of spin up or down electrons [45]. A net spin polarization can be achieved by putting a material in large magnetic field or forcing a system out of equilibrium [34]. In traditional electronics the electron spins are randomly oriented and have no effect on operation and performance of a device, but the novelty of spintronics device is that the currents are

spin polarized and the spin is used to control current flow or store data [25]. Spintronics devices are smaller than 100 nm in size (make it smaller, make it better):large storage capacity per volume, faster operations and less dissipation [18]. The spin polarized in typical semiconductor at room temperature is then lost over distance no longer than a fraction of $0.1\mu m$. This has been the main reason that the development of semiconductor spintronics is closely linked with the advent of nanotechnology and spin dependent phenomena in transport will play any role only when device components reach truly deep-sub-micro dimensions [46]. There are three requirements in spintronics: spin injection, spin manipulation and reliable spin detection [43]. Injecting spin polarized current into semiconductor is not trivial. The manipulation of electron spin along with the charge will open up a faster and more efficient mode of information storage and transfer for quantum computation and communication [44]. The realization of functional spintronics devices requires materials with ferromagnetic ordering at operational temperatures compatible with existing semiconductor materials and being favorable experimental properties, diluted magnetic semiconductors will promisingly suit this need [34]. DMS materials play an irreplaceable role in developing peculiar spintronics devices due to the advantage of simultaneously utilizing the charge and spin of electrons for information processing [47]. In spintronics devices information in stored (written) into spin as particular spin orientation (up or down), where the spins are attached to mobile electrons carry information along the wire and information is read at a terminal [40]. Spin orientation of conduction electrons survives for relatively long time (nanosecond, compared to tens of femtoseconds during which electron momentum decays), which makes spintronics devices particularly attractive for memory storage, magnetic sensor application and potential for quantum computing where electron spin would represent a bit of information [48]. The main goal spintronics is to gain knowledge on spin-dependent phenomena and to exploit them for new functionalities [46].

2.3.2 Advantage of spintronics

The advantages of spin over charge are that spin can be easily manipulated by externally applied magnetic field, a property already in use in magnetic storage technology [41] and more subtle (but potentially significant) property of spin is its long coherence, or relaxation

time-once created it tends to stay that way for along time, unlike charge states, which are easily destroyed by scattering or collision with defects, impurities or other changes [43]. One of the alternative options is the application of another degree of freedom, the spin of the carriers. Already the spintronics plates are used in the field of mass storage devices and have led to compressing massive amounts of data into a small area, at approximately one trillion bits per inch ($1.5 Gbit/mm^2$) [49]. Conventional electronic is based on moving around the electron's charge manipulate it using electric field and the charge of electrons is used to process and store digital information. However, it is now well recognized that further shrinking of physical size of semiconductor electronics will soon approach a fundamental barrier, related electric current leakage, power consumption and heat problems [45]. Engineers and physicists feel the looming presence of quantum mechanics-brilliant physics concept developed in the last century where counterintuitive idea such as spin of electrons, rather than moving charges, spin based devices that would operate by flipping the electron spin orientation would use less energy, generate less heat and would be faster than conventional charge-based devices [39]. This characteristics open the possibility of developing devices that could be much smaller, consume less power and will be more powerful for certain types of computations which is not possible with electron-charge based system [47]. Viewed as whole, the spintronics paradigm offers a variety of potential improvements that include non-volatility, high switching speed, high energy efficiency and the ability to be customized and reconfigured [50].

Chapter 3

Spin Waves and Excitons

3.1 Spin Waves

The concept of spin waves was originally introduced by F. Bloch, who used to explain the temperature dependence of magnetization of ferromagnetic at low temperature [27]. In the low temperature region there are only a few spin waves that are excited and thus their complicated interactions are not so important, this is the best temperature region to examine spin waves [51]. In ferromagnetic materials the lowest energy of the system occurs when all spins are parallel to each other in the direction of magnetization Fig. 3.1a [6]. When one of the spin is tilted or disturbed, how every, it begins to precess- due to the field from the others spins and due to exchange interaction between nearest neighboring disturbance propagates as a wave through the system 3.1b[24]. Spin waves are collective excitations in ordered spin system that consist of propagation of spin deviation, θ from the direction of magnetization of the solid below the critical temperature [52]. As the phonons represent the quanta of collective lattice vibrations in solids, magnons represent the quanta of spin excitations [24].

3.1.1 Exchange Interaction

Exchange interaction arises because of two quantum mechanical spins 1/2 (in isolation), can be in either a spin triplet (total $S = 1$) or singlet (total $S = 0$) [49]. Since the particle carrying the spin are also charged, there will be large energetic difference between the two spin configuration. The energy difference between the singlet and the triplet states ($E_S - E_T$) is the order of electrostatic energy difference, and therefore quite capable of

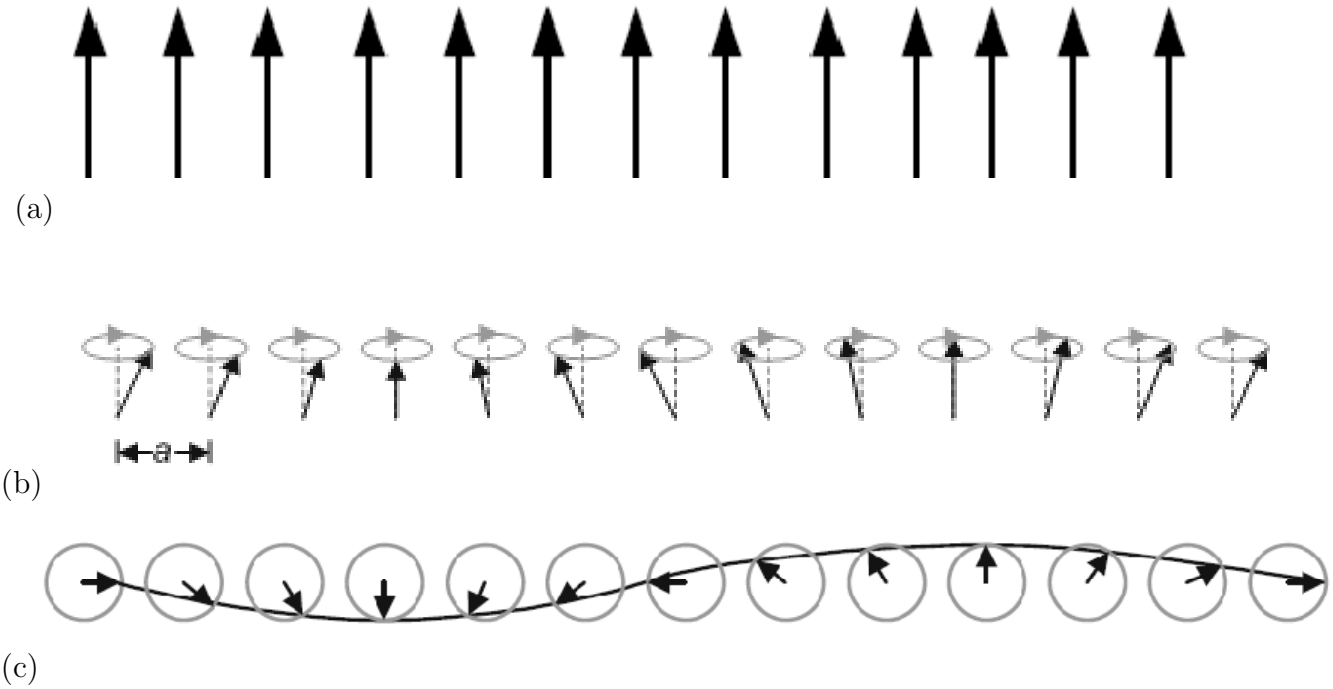

Figure 3.1: Schematic presentation of the orientations of in the row of spin in (a) ferromagnetic in ground state (b) spin wave state viewed from side and (c) viewed from top [6].

being the dominant source of magnetic interaction [51]. The Heisenberg Hamiltonian or a magnetic interaction of the Heisenberg type which expresses the exchange interaction between the electron spins is

$$H = -2j_{12}S_1.S_2 \tag{3.1.1}$$

where J_{12} is known as the exchange coupling constant between Spin 1 and 2 (unit: eV), positive if the interaction is ferromagnetic and negative if it is antiferromagnetic [52]. For the case where several spins interact, we write the total exchange energy as:

$$H = -2\sum_{ij} j_{ij}S_i.S_j \tag{3.1.2}$$

which is Heisenberg Hamiltonian.

3.1.2 Spin Waves In Diluted Magnetic Semiconductors

In magnetic phenomena in solids the important constituent that plays the definitive role is the electron, due to its spin and the associated magnetic moment. For the relevant

theoretical description of spin waves of diluted magnetic semiconductor, the model of dopant spin exchange mediated by holes is utilized. Let us emphasize that in III(Mn)V DMSs the Mn atoms of the magnetic dopants are simultaneously accepter centers where as in II(Mn)VI type DMS, the dopants are no accepters and the holes must be supplied by additional p doping. The important property of the considered system is the randomness of the distribution of magnetic impurity atoms. This random distributions allows for momentum-representation of the collective excitations of the DMS. The low energy excitations of ferromagnetic DMS are a more complicated wave like form, with only slight directional changes between neighboring magnetic moments. A model Hamiltonian which has proved useful in understanding the properties of spin wave in ferromagnetic diluted magnetic semiconductor is the Heisenberg Hamiltonian. In this model the atoms or ions are arranged in a regular lattice position and each of them carries total spin S, and a magnetic moment g$\mu_B S$, where μ_B is the Bohar magneton and g is the Land's g- factor. The Hamiltonian is written as [53]

$$H = -J \sum_{i,j} S_i . S_j - 2\mu_B H_0 \sum_i S_i^z \tag{3.1.3}$$

where H_0 is an external magnetic field along z-direction, J is the measure of the interaction (essentially the exchange interaction) between the two spins at lattice and neighboring lattice and i runs over sites and j runs over nearest neighbors. In ferromagnetic DMSs, with J positive, the ground state is one in which all the spins are aligned in the direction of the external magnetic field [51]. An approximate description of this system in terms of elementary excitations is possible through a transformation originally suggested by Holstein and Primakoff [36]. On the ferromagnetic Heisenberg Hamiltonian Eq. (3.1.3) only nearest neighbors interaction is considered. We assume that which is often realistic that interaction are negligible between spins that are not nearest neighbors, here i and j refer to nearest neighbor lattice sites, S_i . S_j is called an exchanging interaction, and the coefficient J_{ij} are called exchanging constant (which we further assume $J_{ij} = J$) where J is constant and S_i and S_j are operators which have spin components. Although each atom has three components of each spin vector only two of the components are independent.

$$S_i = S_i^x + S_i^y + S_i^z \tag{3.1.4}$$

$$S_j = S_j^x + S_j^y + S_j^z \tag{3.1.5}$$

In this case i and j are site of atoms. From dot product of vectors $A \cdot B = A_x B_x + A_y B_y + A_z B_z$

$$\hat{H} = -J_{ij} \sum_{i,j}, S_i^x S_j^x + S_i^y S_j^y + S_i^z S_j^z - 2\mu_B H_0 \sum_i S_i^z \tag{3.1.6}$$

$$where S_i^x = \frac{1}{2}(S_i^+ + S_i^-), \quad S_j^x = \frac{1}{2}(S_j^+ + S_j^-) \ \ and \ \ S_i^z = S - a_i^+ a_i \tag{3.1.7}$$

where $a_i^+ a_i$ is number operators for bosons and $S_i^+(S_i^-)$ are raisin(powering) spin operators for site i.

$$S_i^y = \frac{1}{2i}(S_i^+ - S_i^-), \quad S_j^y = \frac{1}{2i}(S_j^+ - S_j^-) \ \ and \ \ S_j^z = S - a_j^+ a_j \tag{3.1.8}$$

$$S_i^x S_j^x = \frac{1}{4}\Big[S_i^+ S_j^+ + S_i^+ S_j^- + S_i^- S_j^+ + S_i^- S_j^-\Big] \tag{3.1.9}$$

$$S_i^y S_j^y = \frac{1}{4}\Big[- S_i^+ S_j^+ + S_i^+ S_j^- + S_i^- S_j^+ - S_i^- S_j^-\Big] \tag{3.1.10}$$

$$S_i^z S_j^z = S^2 - S a_j^+ a_j - S a_i^+ a_i + a_i^+ a_i a_j^+ a_j \tag{3.1.11}$$

It will be convenient to rewrite the Hamiltonian in terms of the raising and lowering spin operators.

$$H = \sum_{ij} -J_{ij}\left[\frac{1}{2}[S_i^+ S_j^- + S_i^- S_j^+] + S^2 - S a_j^+ a_j - S a_i^+ a_i + a_i^+ a_i a_j^+ a_j\right] - 2\mu_B H_0 \sum_i S_i^z \tag{3.1.12}$$

where $S_i^- S_j^+$creates or destroy spin deviation on i and j site and $S_i^+ S_j^-$ exchange spin deviation between two sites i and j.

$$\sum_{ij} -J_{ij}\left[\frac{1}{2}[S_i^+ S_j^- + S_i^- S_j^+] + S^2 - S a_j^+ a_j - S a_i^+ a_i\right] - 2\mu_B H_0 \sum_i S_i^z \tag{3.1.13}$$

Term order $a_i^+ a_i a_j^+ a_j$ ignored, because it represents higher order scattering of sine waves which are unimportant at low temperatures. It is much complicated to work with directly

spin operators than creation and annihilation operators. Therefore, it would be advantage if one could represent the spin operators in terms of creation and annihilation operators and work with in stead. We then rewrite the spin operators in the Heisenberg Hamiltonian in terms of boson operators using the Holstein-Primakoff representation which is every useful for studying magnetically ordered state and their excitations [51]. The reason for this is related to the fact that the a_j boson (i.e., the state with no such boson) is the state corresponding to the maximum eigenvalue S of S_j^z. The Holstein- Primakoff representation expressed spin raising and lowering operators on a sites i and j in terms of boson creation and annihilation operators

$$S_i^+ = S_i^x + iS_i^y = (2S)^{1/2}\left(1 - \frac{a_i^+ a_i}{2S}\right)^{1/2} ai \tag{3.1.14}$$

$$S_i^- = S_i^x - iS_i^y = (2S)^{1/2} a_i^+ \left(1 - \frac{a_i^+ a_i}{2S}\right)^{1/2} \tag{3.1.15}$$

where $a_i^+ a_i$ and $a_j^+ a_j$ are the number operators for sites i and j, i.e., they count the number of bosons on i and j sites respectively. The a_i^+ and a_j^+ creates spin deviations at sites i and j respectively.

$$f(x) = f(0) + \frac{f^{'}(0)x}{1!} + \frac{f^{''}(0)x^2}{2!} + ... \tag{3.1.16}$$

Let $x = \frac{a_i^+ a_i}{2S}$ and $f(x) = (1-x)^{1/2}$

$$f(0) = 1, f^{'}(x) = -\frac{1}{2}(1-x)^{-1/2}, f^{''}(x) = -\frac{1}{4}(1-x)^{-3/2} + ... \tag{3.1.17}$$

Equation (3.1.16) becomes

$$f(x) = 1 - \frac{x}{2} - \frac{x^2}{8} + ... \tag{3.1.18}$$

Equations 3.1.14 and 3.1.15 become

$$\hat{S}_i^+ = (2S)^{1/2}\left(1 - \frac{a_i^+ a_i}{4S} - \frac{(a_i^+ a_i)^2}{32S^2} + ...\right) a_i \tag{3.1.19}$$

$$\hat{S}_i^- = (2S)^{1/2}\left(1 - \frac{a_i^+ a_i}{4S} - \frac{(a_i^+ a_i)^2}{32S^2} + ...\right) a_i^+ \tag{3.1.20}$$

This implies that the relation between the S and a in i and j sites can be approximated by

$$S_i^+ = (2S)^{1/2} a_i \qquad S_j^+ = (2S)^{1/2} a_j \tag{3.1.21}$$

$$S_i^- = (2S)^{1/2} a_i^+ \qquad S_j^- = (2S)^{1/2} a_j^+ \tag{3.1.22}$$

The higher order terms $a_i^+ a_i a_i$, $a_i^+ a_i a_i^+, a_i^+ a_i a_i^+ a_i$ and $a_i^+ a_i a_i^+ a_i a_i^+$ are ignored due to scattering. By substituting Eq.(3.1.21) and (3.1.22) in to Eq.(3.1.13), the result is

$$H = \sum_{ij} -J_{ij} S \Big[a_i a_j^+ + a_i^+ a_j + S - a_j^+ a_j - a_i^+ a_i \Big] - 2\mu_B H_0 N S + 2\mu_B H_0 \sum_i a_i^+ a_i \tag{3.1.23}$$

$$H = \sum_{ij} -J_{ij} S^2 - 2\mu_B H_0 N S + \sum_{ij} -J_{ij} S \Big[a_i a_j^+ + a_i^+ a_j - a_j^+ a_j - a_i^+ a_i \Big] + 2\mu_B H_0 \sum_i a_i^+ a_i \tag{3.1.24}$$

$$\hat{H} = H^{'} + H^{magnon} \tag{3.1.25}$$

$H^{'}$ will not change the dynamics of the system because it has no spin wave variables.

$$H^{magnon} = \sum_{ij} -J_{ij} S \Big[a_i a_j^+ + a_i^+ a_j - a_j^+ a_j - a_i^+ a_i \Big] + 2\mu_B H_0 \sum_i a_i^+ a_i \tag{3.1.26}$$

The terms in the square bracket are operators expressing explicitly the handing on of spin deviations from one site to the next. Since the spin deviations are not localized to particular lattice site but propagates throughout we need the creation operators that create non-localized excitations through the sample. The transformation that will do this is Fourier transformation variables for boson operators, which are given by [54]

$$a_i = \frac{1}{\sqrt{N}} \sum_k e^{-ik.ri} b_k \;\; and \;\; a_i^+ = \frac{1}{\sqrt{N}} \sum_k e^{ik.ri} b_k^+ \tag{3.1.27}$$

$$a_j = \frac{1}{\sqrt{N}} \sum_k e^{-ik.rj} b_k \;\; and \;\; a_j^+ = \frac{1}{\sqrt{N}} \sum_k e^{ik.rj} b_k^+ \tag{3.1.28}$$

where k is magnon wave vector, b_k is magnon creation operator, b_k^+ is magnon annihalation operator, N is number of lattice and since we considering nearest neighbor interaction we

can write $r_j = r_i + \delta$, where δ is vector connecting nearest neighbor sites, r_j and r_i are electron coordinates. Spins locally deviate only by a small amount from their ground state values parallel to z-axis as spin wave passed by. The total number of magnons equals the total spin deviation quantum number. The commutation relation b_k obey the same kind of commutation relation as the original boson operators a_j, i.e., $[b_k, b_{k'}^+]$=$\delta_{kk'}$. So there are as many operators b_k as there are operators a_j.

$$H^{mag} = -JS\sum_{ij}\left[\frac{1}{\sqrt{N}}\sum_k e^{-ik.r_i}b_k.\frac{1}{\sqrt{N}}\sum_{k'} e^{ik'.r_j}b_{k'}^+ + \frac{1}{\sqrt{N}}\sum_k e^{ik.r_i}b_k^+\frac{1}{\sqrt{N}}\sum_{k'} e^{-ik'.r_j}b_{k'} - \frac{1}{\sqrt{N}}\sum_k e^{ik.r_j}b_k^+\frac{1}{\sqrt{N}}\sum_{k'} e^{-ik'.r_j}b_{k'} - \frac{1}{\sqrt{N}}\sum_k e^{ik.r_i}b_k^+\frac{1}{\sqrt{N}}\sum_{k'} e^{-ik'.r_i}b_{k'}\right] + 2\mu_B H_0\sum_i \frac{1}{\sqrt{N}}\sum_k e^{ik.r_i}b_k^+\frac{1}{\sqrt{N}}\sum_{k'} e^{-ik'.r_i}b_{k'} \tag{3.1.29}$$

$$H^{mag} = \frac{-JS}{N}\sum_{i\delta k,k'}\left[e^{-ik.r_i}b_k e^{ik'(r_i+\delta)}b_{k'}^+ + e^{ik.r_i}b_k^+ e^{-ik'(r_i+\delta)}b_{k'} - e^{ik(r_i+\delta)}b_k^+ e^{-ik'(r_i+\delta)}b_{k'} - e^{ik.r_i}b_k^+ e^{-ik'.r_i}b_{k'}\right] + \frac{1}{N}2\mu_B H_0\sum_{ikk'} e^{ik.r_i}b_k^+ e^{-ik'.r_i}b_{k'} \tag{3.1.30}$$

$$H^{mag} = \frac{-JS}{N}\sum_{i\delta k,k'}\left[e^{-i(k-k')ri}e^{ik'.\delta}b_k b_{k'}^+ + e^{i(k-k')ri}e^{-ik'.\delta}b_k^+ b_{k'} - e^{i(k-k')r_i}e^{i(k-k')\delta}b_k^+ b_{k'} - e^{i(k-k')ri}b_k^+ b_{k'}\right] + \frac{1}{N}2\mu_B H_0\sum_{ikk'} e^{i(k-k')ri}b_k^+ b_{k'} \tag{3.1.31}$$

$$By\ using\quad \sum_i e^{i(k-k')ri} = N, for k = k' \tag{3.1.32}$$

$$H^{mag} = \sum_k\left[-JS\left(\sum_\delta e^{ik'.\delta}b_k b_{k'}^+ + \sum_\delta e^{-ik'.\delta}b_k^+ b_{k'} - b_k^+ b_{k'} - b_k^+ b_{k'}\right) + 2\mu_B H_0 b_k^+ b_{k'}\right] \tag{3.1.33}$$

we use

$$\gamma_k = \frac{1}{z}\sum_\delta e^{ik'.\delta}\ and\ \gamma_{-k} = \frac{1}{z}\sum_\delta e^{-ik'.\delta} \tag{3.1.34}$$

are the magnon function, which in the approximation depends only on the positions of the nearest neighbor spins

$$H^{mag} = \sum_k\left[-JSz\left(\gamma_k b_k b_{k'}^+ + \gamma_{-k}b_k^+ b_{k'} - 2b_k^+ b_{k'}\right) + g\mu_B H_0 b_k^+ b_{k'}\right] \tag{3.1.35}$$

$$H^{mag} = \sum_k \Bigg[- JSz\Big(\gamma_k(1 + b_k^+ b_k^+) + \gamma_{-k} b_k^+ b_{k'} - 2b_k^+ b_{k'}\Big) + g\mu_B H_0 b_k^+ b_{k'}\Bigg] \tag{3.1.36}$$

$$H^{mag} = \sum_k \Bigg[- JSz\Big(\gamma_k + \gamma_k b_k^+ b_k + \gamma_{-k} b_k^+ b_{k'} - 2b_k^+ b_{k'}\Big) + g\mu_B H_0 b_k^+ b_{k'}\Bigg] \tag{3.1.37}$$

$$H^{mag} = -JSz \sum_k \gamma_k - JSz \sum_k \Big[\gamma_k b_k^+ b_k + \gamma_{-k} b_k^+ b_{k'} - 2b_k^+ b_{k'} + g\mu_B H_0 b_k^+ b_{k'}\Big] \tag{3.1.38}$$

$$H^{mag} = -JSz \sum_k \Big[2\gamma_k b_k b_{k'}^+ - 2b_k^+ b_{k'}\Big] + g\mu_B H_0 \sum_k b_k^+ b_{k'}\Bigg] \tag{3.1.39}$$

We note that $\sum_k \gamma_k = 0$ *and* $\gamma_k = \gamma_{-k}$ if there is a center of symmetry.

$$H^{mag} = \sum_k \Bigg[- 2JSz\gamma_{-k} + 2JSz + g\mu_B H_0\Bigg] b_k^+ b_k \tag{3.1.40}$$

$$H^{mag} = \sum_k \Big[2JSz(1 - \gamma_{-k}) + g\mu_B H_0\Big] b_k^+ b_k \tag{3.1.41}$$

At low temperature spin waves approximation that they are harmonic oscillator or phonon type Hamiltonian. Under this assumption, the magnon part of the Hamiltonian can be simply written as $H = \sum_k \hbar\omega_k b_k^+ b_k$. ($\hbar = 1$)

$$\omega_k = 2JSz(1 - \gamma_k) + g\mu_B H_0 \tag{3.1.42}$$

is the magnon dispersion where z is the nearest neighbor spins. As an example, let us consider the case of simple cubic lattice in 3D. In this case, the nearest neighbors(z=6) are along the $\pm X, \pm Y and \pm Z$ axes at distance a and we have

$$\gamma_k = \frac{1}{3}\Big(cosk_x a + cosk_y a + cosk_z a\Big) \tag{3.1.43}$$

From Eq. (3.1.42) above, $1 - \gamma_k$ is given by

$$1 - \gamma_k = 1 - \frac{cosk_x a + cosk_y a + cosk_z a}{3} = \frac{1 - coska}{3} \tag{3.1.44}$$

where, k_x+k_y+k_z=k. When 1- coska expands, it becomes $\frac{k^2a^2}{2}$ and, for $ka << 1$, it is $\cong k^2a^2$. Averaging over the impurities or considering total spin in the sample, Eq. (3.1.42) becomes

$$\omega_k = \frac{2}{3} x_m JSz k^2 a^2 + g\mu_B H_0 \tag{3.1.45}$$

$$\omega_k = Ak^2 + g\mu_B H_0 \tag{3.1.46}$$

where A=$\frac{2}{3}x_m JSza^2$. In this case ferromagnetic ordering is considered where the externally applied field is very small and negligible, so that H_0 is taken to be zero. Thus,

$$\omega_k = Ak^2 \tag{3.1.47}$$

which implies $\omega_k \propto k^2$(parabolic wave vector dispersion)

3.2 Exciton

An exciton can be formed when a photon is absorbed by a semiconductor and excites an electron from valance band into conduction band [41]. The photon-excited electron that failed to reach the conduction band as shown in Fig.3.5, bounds togather with the hole left behind by attractive coulomb interaction to form state known as exciton. Alternatively, exciton may be an excited state of an atom, ion or molecules, that excite from one cell of the lattice to another [6]. This particle is important to describe optical properties of bulk semiconductor and structure, specially at low temperature [54]. An exciton can move through the crystal and transport energy, it does not transport charge because it is electrically neutral. Excitons are unstable with respect to the ultimate recombination process in which the electron drops into the hole [6]. Excitons are the main mechanism for light emission in semiconductor at low temperatures (when the characteristics thermal energy $k_B T$ is less than the exciton binding energy). At high temperatures the mechanism for light emission is the recombination of free electrons and holes. A free electron and hole created whenever a photon of energy greater than the energy gap ($\hbar\omega > Eg$) is absorbed in crystal. Excitons are approximately bosons and their life time is actually short (of the order of nanoseconds or shorter) due to recombination of the electron and hole [55].

3.2.1 Types of Excitons

The study of excitons was pioneered by Frenkel and Winnier in the 1930s. Consequently, this quasi-particle is nowadays classified according to where the electron and hole are bound strongly (Frenkel exciton) or bound weakly (Wannier exciton) [56].

3.2.2 Frenkel Excitons

In materials with small dielectric constant, the coulomb interaction between electron and hole may be strong and the excitons tend to be small of the same order as the size of the lattice constant [54]. The Frenkel excitons is highly localized and is often found in

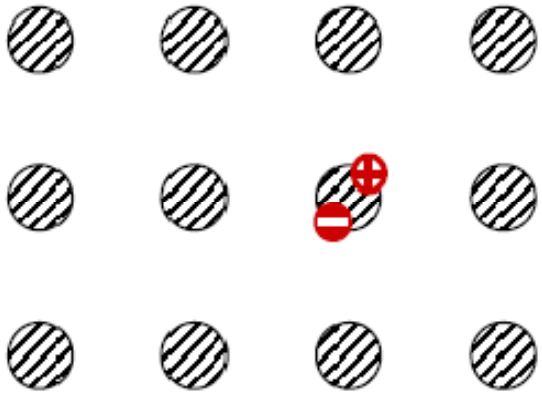

Figure 3.2: Molecular picture: tightly bound electron-hole pair or Frenkel exciton where the hole is localized on one atom but, the electron is always close to the hole [57].

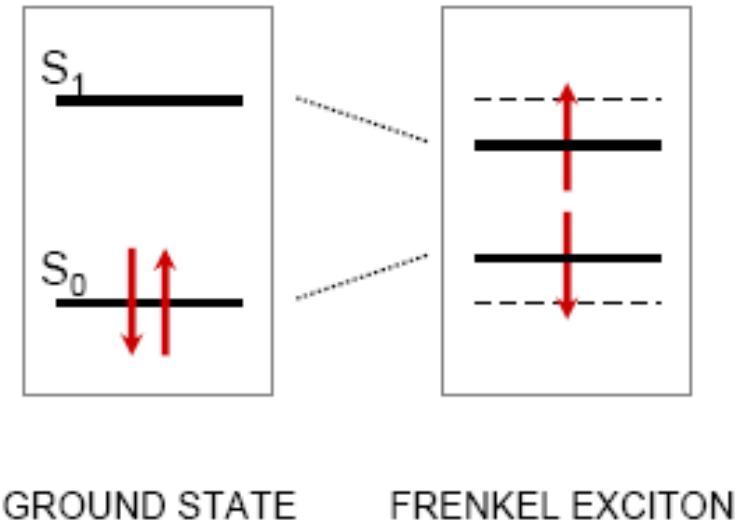

Figure 3.3: Ground and excited electronic states of Frenkel exciton. Binding energy $\approx 1meV$ and radius $\approx 10A^0$ [57].

molecular solids where molecules are not densely packed [57] and are localized on one lattice site or an other way to view Frenkel excitons is as a propagating excited state

of a single atom, but the excitation can hop from one atom to another by virtue of the coupling between neighbors. Frenkel excitons are typically found in alkali halide crystals composed aromatic molecules such as anthracene and tetracene [57]. The Frenkel exciton are obtained when both (+) and (-) occupy essentially the same molecular site as shown in the Fig. 3.2. We can consider excitons in another way according to their spin. In the Fig. 3. 3, in singlet state opposite spins are there. After excitation the two electrons may have a correlation between the lower and upper electronic states and we can now consider two excitation states. One where the electron in the upper state has the same spin as the vacant electron in the lower state and the second where the electron spin in the upper state has an opposite spin. The excitation in the second case requires a spin flip (momentum) and the material is not optically active [58].

3.2.3 Mott-Wannier Excitons

Wannier-Mott excitons are typically found in semiconductor crystals with small energy gaps, high dielectric constants and have a Bohr radius much larger than intera-atomic spacing of a crystal because the medium is dense (like in crystal) then the atoms screen some of the e-h attraction and the exciton size spread into large space as in the Fig. 3.4 and have small binding energies and move quit freely through the crystal [59]. Electric field screening due to the large dielectric constant reduces the Coulomb interaction between electrons and holes ($\frac{e^2}{\varepsilon r}$), where r is the distance between the particles and ε is the appropriate dielectric constant of a semiconductor. Thus the Bohr radius of Wannier-Mott excitons are much larger compared to the one of Frenkel. Generally, Wannier-Matt excitons are typically found in semiconductor crystals with small energy gap and high dielectric constants, but have also been identified in liquids, such as liquid xenon [60]. As the transitions within the ground multiples of the magnetic ions which give rise to magnons, there are transition of higher levels, which give to rise excitons [49]. We assume that exciton dispersion is negligible, and denote the exciton energy by β_k which is wave vector k' dependence. Thus the exciton Hamiltonian can be written as [56].

$$H^{ex} = \sum_i \beta_{k'} c_i^+ c_i \tag{3.2.1}$$

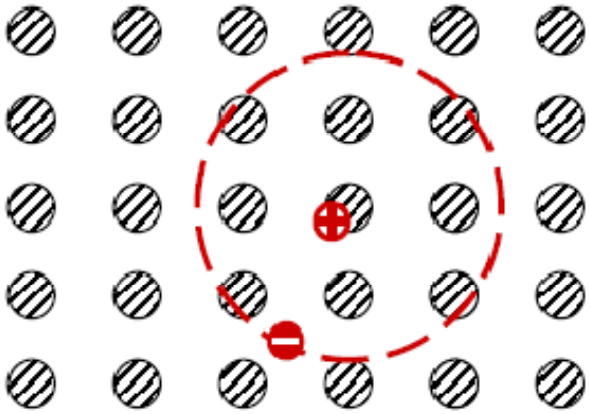

Figure 3.4: The exciton shown is Matt-Wannier excitons: it is weakly bound with an average electron-hole distance larger in comparison with the lattice constant [6].

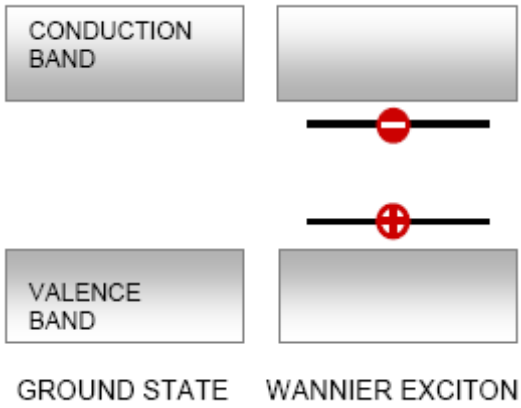

Figure 3.5: Ground and excited electronic states of Wannier exciton. Binding energy $\sim 10meV$ and radius $\sim 100A^0$ [60].

where c_i^+creates an exciton on the i^{ih} site. Excitons are quasi-particles in the solids which have generally mass of hole much larger than the electron mass, the two bodies system is similar to hydrogen atom, but different in mass. From the well known solution to the hydrogen atom problem. The bound states of the exciton system having total energies lower than the bottom of the conduction band [6]. The energy level is given by

$$E_n = E_g - \frac{\mu e^4}{2\hbar^2 \epsilon^2 n^2} \tag{3.2.2}$$

where e is the free electron charge, ϵ is dielectric constant, E_n is the exciton energy levels Fig 3.6, n is principal quantum number which n = 1, 2, 3..., E_g is band gap energy, the

last term is exciton Rydberg equation and $\frac{1}{\mu} = \frac{1}{m_e^*} + \frac{1}{m_h^*} \Rightarrow \mu = \frac{m_e^* m_h^*}{m_e^* + m_h^*}$ is the reduced mass where m_e^* and m_h^* are effective mass of electron and hole respectively.

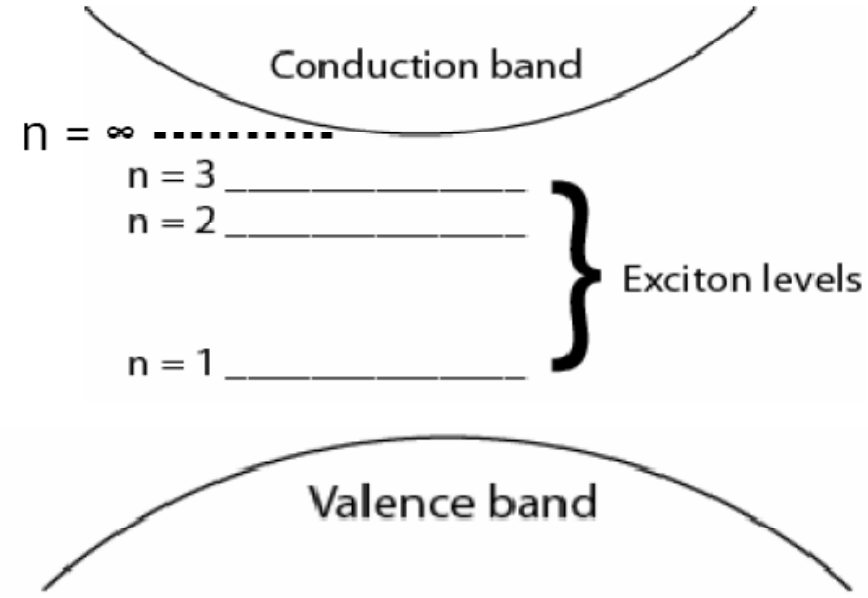

Figure 3.6: The exciton energy levels[61].

Chapter 4

Mathematical Technique

4.1 Green Function Formalism

The Green functions play important part in the field theoretical treatment of the many body problem and are powerfull when combined with spectra representations and also thermodynamic properties are derived from them [51]. In Quantum field theory the Green functions are the so-called propagators. The name is given because in order to find the physical properties of a system, it is essential to know, not the detailed behavior of each particle in the system but rather just the average behavior of one or two typical particles. So, propagators are the basic quantities that describe the average behavior [27]. Propagation from one point to another in quantum mechanics in generally expressed in terms of transmission amplitudes. So, Green function contains information about the transmission amplitude for the particle. There are different Green functions or propagators: One-particle, two-particle, n-particles, advanced and retarded. The single-particle propagator G is a sum of probability amplitudes for all the way of going from r_1, t_1 to r_2, t_2 . The propagator G yields directly the energies, life-time of the quasi-particles, momentum distribution, the spin, the particle density and used to calculate ground state energy [50]. The two-particle propagator G_2 is the sum of the probability amplitudes for all the way two particles can enter a system, undergo interactions and emerge again. The two-particle propagator G_2 gives directly, energy, the life-time of collective excitations, magnetic susceptibility and the electrical conductivity [60]. The term "advanced" means that it gives the state of the system at previous times based on the state of the system at the present time. The retarded one, gives the present state of the system as it has

evolved from the state at the previous times i.e., the effect of retardation [62]. The solution for the two Green function are however, subjected to different boundary conditions: $Gr(t,t') = 0 \quad for\ t < t'$ and $Ga(t,t') = 0 \quad for \quad t > t'$ and green function is not defined for t = t'

4.1.1 The Double-Time Temperature Dependent Green Function

The method of the double-time temperature dependent Green functions in statistical mechanics are the appropriate generalization of the correlation functions. They are useful in calculating the average of dynamical quantities, and they have great advantages when equations are formed and solved [35]. Actually calculating the Green function G(t, t') for the double-time- temperature dependent Green function can be done via the general equation of motion for Heisenberg operators A(t) and B(t'). The retarded Green function Gr(t, t') is given by

$$Gr(t,t') \equiv \langle\langle A(t); B(t')\rangle\rangle r = -i\theta(t-t')\langle[A(t), B(t')]_{r\pm}\rangle \tag{4.1.1}$$

and advanced Green function Ga(t,t') is

$$Ga(t,t') \equiv \langle\langle A(t); B(t')\rangle\rangle_a = i\theta(t-t')\langle[A(t), B(t')]_{a\pm}\rangle \tag{4.1.2}$$

From the above, the notations $\langle\langle ...\rangle\rangle_r$, are corresponding Green functions, single pointed bracket $\langle ...\rangle$ represents the thermal average over a canonical ensemble which is appropriate since the number of particles is not constant, square bracket $[.., ..]_-$ is the usual commutator, $[.., ..]_+$ is anticommutator which used in Fermionic system in Green function occurring in a certain problems. So, A(t) and B(t') are either Fermion or Boson operators and correspondingly the commutation, $[A(t), B(t')]_\pm = A(t)B(t') \pm B(t')A(t)$ [63] and $\theta(t-t)$ is the Heaviside step function having the property

$$\theta(t-t') = 1, for\ (t-t') > 0 \quad and \quad 0, for\ (t-t') < 0 \tag{4.1.3}$$

The Eq. (4.1.1) and Eq. (4.1.2) can be written as

$$Gr(t,t') \equiv \langle\langle A(t); B(t')\rangle\rangle_r = -i\theta(t-t')\rangle A(t)B(t') \pm B(t')A(t)\rangle \tag{4.1.4}$$

$$Ga(t,t') \equiv \langle\langle A(t); B(t')\rangle_a = i\theta(t-t')\langle A(t)B(t') \pm B(t')A(t)\rangle \tag{4.1.5}$$

The Green functions will not depend on t and t' separately, but only on the difference t-t'. When the times are different ($t \neq t'$), these averages yield the time correlation function which are essential for transport processes. This time-correlation function like Green function depend on the time difference (t - t').

4.1.2 The Equation of Motion of Green Function

By differentiating the retarded Green function Gr(t, t') given by Eq. (4.1.1) and advanced Green function Ga (t, t') by Eq. (4.1.2) with respect to time, we can derive the equation of motion of Green function. In this schem one uses a retarded double-time Green function which is given by

$$Gr(t,t') \equiv \langle\langle A(t); B(t')\rangle\rangle = -i\theta(t-t)\langle[A(t), B(t')]\rangle_- \tag{4.1.6}$$

$$\frac{d}{dt}\langle\langle A(t); B(t')\rangle\rangle = \frac{d}{dt}\Big[- i\theta(t-t')\langle[A(t), B(t')]\rangle\Big] \tag{4.1.7}$$

multiplying both ide by i

$$\frac{id}{dt}\langle\langle A(t); B(t')\rangle = \frac{id}{dt}\Big[- i\theta(t-t^{'})\langle[A(t), B(t')]\rangle\Big] \tag{4.1.8}$$

$$= \frac{d}{dt}\theta(t-t^{'})\langle[A(t), B(t')]\rangle - i\theta(t-t^{'})\langle[\frac{id}{dt}A(t), B(t')]\rangle \tag{4.1.9}$$

The last right part of he eqution above is a Green function and Eq. (4.1.9) becomes

$$\frac{id}{dt}\langle\langle A(t); B(t^{'})\rangle\rangle = \frac{d}{dt}\theta(t-t^{'})\langle[A(t), B(t')]\rangle + \langle\langle\frac{id}{dt}A(t); B(t^{'}\rangle\angle \tag{4.1.10}$$

We have

$$\frac{d}{dt}\theta(t-t') = \delta(t-t') = \frac{d}{dt'}\theta(t-t') \tag{4.1.11}$$

From Heisenberg picture, A(t) and B(t') satisfy equation of the form

$$\frac{idA(t)}{dt} = [A(t), \hat{H}] \tag{4.1.12}$$

By sustituting Eq.(4.1.11) and Eq. (4.1.12) into Eq. (4.1.10)

$$\frac{id}{dt}\langle\langle A(t);B(t')\rangle = \delta(t-t^{'})\langle[A(t),B(t')]\rangle + \langle\langle[A(t),H];B(t')\rangle\rangle \tag{4.1.13}$$

To solve Eq. (4.1.13) it is conveneint to work with the Fourier transformation of this equation. Substituting for Green function which is given by

$$G(t,t') = \langle\langle A(t);B(t')\rangle\rangle = \int_{-\infty}^{\infty} dEG(E)e^{-iE(t-t')} \tag{4.1.14}$$

In addition, the delta function can be defined as

$$\delta(t-t') = \frac{1}{2\pi}\int_{-\infty}^{\infty} dEe^{-iE(t-t')} \tag{4.1.15}$$

Eq. (4.1.13) becomes

$$E\int_{-\infty}^{\infty} dEG(E)e^{-iE(t-t')} = \frac{1}{2\pi}\int_{-\infty}^{\infty} dEe^{-iE(t-t')}\langle[A(t),B(t^{'})]\rangle + \langle\langle[A(t),H];B(t')\rangle\rangle \tag{4.1.16}$$

The Fourier transform of Eq. (4.1.16) can be obtained by multplying its both sides by

$$\frac{1}{2\pi}\int_{-\infty}^{\infty} dte^{i\omega(t-t')} \tag{4.1.17}$$

$E\int_{-\infty}^{\infty} dEG(E)\frac{1}{2\pi}\int_{-\infty}^{\infty} dte^{i(\omega-E)(t-t')} = \frac{1}{2\pi}\int_{-\infty}^{\infty} dE\frac{1}{2\pi}\int_{-\infty}^{\infty} e^{i(\omega-E)(t-t')}dt\langle[A(t),B(t')]\langle$

$$+F.Tof\langle\langle[A(t),H];B(t)\rangle\rangle \tag{4.1.18}$$

By using Fourier integeral theorem

$$\frac{1}{2\pi}\int_{-\infty}^{\infty} e^{i(\omega-E)(t-t^{'})}dt = \delta(\omega-E) \tag{4.1.19}$$

Eq. (4.1.18) could be written as

$$E\int_{-\infty}^{\infty} G(E)\delta(\omega-E)dE = \frac{1}{2\pi}\int_{-\infty}^{\infty}\delta(\omega-E)dE\langle[A(t),B(t')]\rangle + \langle\langle[A()t,H];B(t')\rangle\rangle \tag{4.1.20}$$

From propertis of Dirc delta function $\int_{-\infty}^{\infty}\delta(x)dx = 1$. Therefore, for $\omega = E, \delta(\omega-E)dE =$ 1 more simplified form of Eq. (4.1.20) is

$$EG(E) = \frac{1}{2\pi}\langle[A(t),B(t')]\rangle + \langle\langle[A(t),H];B(t')\rangle\rangle \tag{4.1.21}$$

This shows the delta function and constant $\frac{1}{2\pi}$ are Fourier transfom of each other. G(E) is Fouries transform of G(t-t'), we can write Eq.(4.1.21) as

$$EG(E) = E\langle\langle A(t); B(t')\rangle\rangle = \frac{1}{2\pi}\langle[A(t), B(t')]\rangle + \langle\langle[A(t), H]; B(t')\rangle\rangle \tag{4.1.22}$$

which is equation of motion of Green function, where E can be dispertion energy of magnon or like the one that we are studying.

Chapter 5

Exciton-Magnon Interaction

5.1 The Model Hamiltonian

The model consists of magnon, exciton and magnon-exciton interaction energies, written as

$$H = H^{mag} + H^{ex} + H^{mag-ex} \tag{5.1.1}$$

where H^{mag} is free magnon energy, H^{ex} is free exciton energy, and H^{mag-ex} is the interaction energy, thus the standard model Hamiltonian of the system can be rewritten as

$$H = \sum_{k} \omega_k b_k^+ b_k + \sum_{k'} \beta_{k'} c_{k'}^+ c_{k'} + \sum_{k,k'} \Theta_{k,k'} \left[b_k^+ c_{k'} + c_{k'}^+ b_k \right] \tag{5.1.2}$$

The operators $b_k^+(b_k)$ and $c_{k'}^+(c_{k'})$ are creation (annihilation) operators for magnon and exciton respectively, while ω_k is magnon energy, $\beta_{k'}$ is exciton energy and Θ is magnon-exciton interaction energy which is assumed as independent of the propagation wave vector, $\vec{k}$.

5.2 The Equation of Motion

Since magnons are the excitations associated with transverse spin components, the Green function contain a full description of the dynamic behavior of the magnetic system, and can be employed to evaluate the dynamic properties of the magnon or the intensities of the magnons. To find the average number and dispersion of the system, the Green function

formulism is employed. This would be done by using the equation of motion given by

$$\varepsilon_k\langle\langle b_k; b_k^+\rangle\rangle = \frac{1}{2\pi}\langle[b_k, b_k^+]\rangle + \langle\langle[b_k, H]; b_k^+\rangle\rangle \tag{5.2.1}$$

$\langle\langle[b_k, H]; b_k^+\rangle\rangle$ in terms of $\langle\langle b_k; b_k^+\rangle\rangle$ by some decoupling approximation. By substituting the model Hamiltonian of Eq.(5.1.2) in to Eq.(5.2.1),

$$\varepsilon_k\langle\langle b_k; b_k^+\rangle\rangle = \frac{1}{2\pi}\langle[b_k, b_k^+]\rangle + \langle\langle[b_k, \sum_k \omega_k b_k^+ b_k + \sum \beta_{k'} c_{k'}^+ c_{k'} + \sum_{k,k'} \Theta(b_k^+ c_{k'} + c_{k'}^+ b_k)]; b_k^+\rangle\rangle \tag{5.2.2}$$

In the following we assume the case of magnon and exciton weak interaction to be elastic type of scattering with equal magnitude of wave vector, hence, $\mid \vec{k'} \mid = \mid \vec{k} \mid = k$, The subscript k in Hamiltonian is replaced by p simply to avoid confusion. Let us first handle the Hamiltonian part.

$$[b_k, H] = [b_k, \sum_p \omega_p b_p^+ b_p + \sum_p \beta_p c_p^+ c_p + \sum_p \Theta(b_p^+ c_p + C_p^+ b_p)] \tag{5.2.3}$$

$$= [b_k, \sum_p \omega_p b_p^+ b_p] + [b_k, \sum_p \beta_p c_p^+ c_p] + [b_k, \sum_p \Theta(b_p^+ c_p + c_p^+ b_p)] \tag{5.2.4}$$

For all operators A, B and C, [A,BC]=[A,B]C + B[A,C] or using $[b_i, b_j]$ *and* $[b_i^+, b_j^+]$ is equal to zero.

$$= \textstyle\sum_p \omega_p \Big([b_k, b_p^+] b_p + b_p^+ [b_k, b_p] \Big) + \sum_p \beta_p \Big([b_k, c_p^+] c_p + c_p^+ [b_k, c_p] \Big) +$$

$$\sum_k \Theta \Big([b_k, b_p^+] c_p + b_p^+ [b_k, c_p] + [b_k, c_p^+] b_p + c_p^+ [b_k, b_p] \Big) \tag{5.2.5}$$

$$= \omega_p \sum_p \delta_{k,p} b_p + \sum_p \Theta \delta_{p,k} c_p \tag{5.2.6}$$

The commutation relation solved by using $[b_i, b_j^+] = \delta_{ij}, \delta_{ij} = 1$ if $i = j$, otherwise zero. Since $p = k$, the Eq (5.2.6) becomes

$$[b_k, H] = \omega_k b_k + \Theta c_k \tag{5.2.7}$$

substituting Eq. (5.2.7) in to Eq. (5.2.1), for$[b_k, H]$ we obtain

$$\varepsilon_k\langle\langle b_k; b_k^+\rangle\rangle = \frac{1}{2\pi}\langle[b_k, b_k^+]\rangle + \langle\langle \omega_k b_k + \Theta c_k; b_k^+\rangle\rangle \tag{5.2.8}$$

$$= \frac{1}{2\pi} + \omega_k \langle\langle b_k, b_k^+ \rangle\rangle + \Theta \langle\langle c_k; b_k^+ \rangle\rangle \tag{5.2.9}$$

$$(\epsilon_k - \omega_k)\langle\langle b_k, b_k^+ \rangle\rangle = \frac{1}{2\pi} + \Theta \langle\langle c_k; b_k^+ \rangle\rangle \tag{5.2.10}$$

Following similar procedure we can write the equation of motion for $\langle\langle c_k; b_k^+ \rangle\rangle$

$$\varepsilon_k \langle\langle c_k; b_k^+ \rangle\rangle = \frac{1}{2\pi}\langle [c_k, b_k^+] \rangle + \langle\langle [c_k, H]; b_k^+ \rangle\rangle \tag{5.2.11}$$

By substituting the Hamiltonian on Eq. (5.2.1) into Eq.(5.2.11),

$$\begin{aligned}
[c_k, H] &= [c_k, \sum_p \omega_p b_p^+ b_p + \sum_p \beta_p c_p^+ c_p + \sum_p \Theta(b_p^+ C_p + c_p^+ b_p)] \\
&= [c_k, \sum_p \omega_p b_p^+ b_p] + [c_k, \sum_p \beta_p c_p^+ c_p] + [c_k, \sum_p \Theta(b_p^+ c_p + c_p^+ b_p)] \\
&= \sum_p \omega_p \Big([c_k, b_p^+] b_p + b_p^+ [c_k, b_p] \Big) + \sum_p \beta_p \Big([c_k, c_p^+] c_p + c_p^+ [c_k, c_p] \Big) \\
&+ \sum_p \Theta \Big([c_k, b_p^+] c_p + c_p^+ [c_k, c_p] + [c_k, c_p^+] b_k + c_p^+ [c_k, b_k] \Big)
\end{aligned} \tag{5.2.12}$$

The above equation is simplified to

$$[c_k, H] = \beta_k c_k + \Theta b_k \tag{5.2.13}$$

By substituting Eq.(5.2.13) into Eq. (5.2.11)

$$\varepsilon_k \langle\langle c_k; b_k^+ \rangle\rangle = \beta_k \langle\langle c_k; b_k^+ \rangle\rangle + \Theta \langle\langle b_k; b_k^+ \rangle\rangle \tag{5.2.14}$$

$$\langle\langle c_k; b_k^+ \rangle\rangle = \frac{\Theta \langle\langle b_k; b_k^+ \rangle\rangle}{\varepsilon_k - \beta_k} \tag{5.2.15}$$

By substituting Eq.(5.2.15) into Eq. (5.2.10) we obtain

$$(\epsilon_k - \omega_k)\langle\langle b_k; b_k^+ \rangle\rangle = \frac{1}{2\pi} + \frac{\Theta^2 \langle\langle b_k; b_k^+ \rangle\rangle}{\epsilon_k - \beta_k} \tag{5.2.16}$$

$$\left(\varepsilon_k - \omega_k - \frac{\Theta^2}{\varepsilon_k - \beta_k} \right) \langle\langle b_k; b_k^+ \rangle\rangle = \frac{1}{2\pi} \tag{5.2.17}$$

$$\langle\langle b_k; b_k^+ \rangle\rangle = \frac{1}{2\pi \left(\varepsilon_k - \omega_k - \frac{\Theta^2}{\varepsilon_k - \beta_k} \right)} \tag{5.2.18}$$

Poles of Green functions are singularities that occur only on the real axis and show energy absorbed or released in particle transfer [61]. The pole of the Green function Eq.(5.2.18) would be at

$$2\pi\left(\varepsilon_k - \omega_k - \frac{\Theta^2}{\varepsilon_k - \beta_k}\right) = 0 \Rightarrow \varepsilon_k = \omega_k + \frac{\Theta^2}{\varepsilon_k - \beta_k} \tag{5.2.19}$$

By rearranging solving for ε_k

$$\varepsilon_k(\varepsilon_k - \beta_k) - \omega_k(\varepsilon_k - \beta_k) - \Theta^2 = 0 \tag{5.2.20}$$

$$\varepsilon_k^2 - (\beta_k + \omega_k)\varepsilon_k + \omega_k\beta_k - \Theta^2 = 0 \tag{5.2.21}$$

Let us ε_k =x, $\beta_k + \omega_k$ = b and $\omega_k\beta_k - \Theta^2$ = c, we get quadratic equation form and its solution is, $x = \frac{-b \pm \sqrt{b^2 - 4ac}}{2a}$

$$\varepsilon_k = \frac{\beta_k + \omega_k}{2} \pm \frac{1}{2}\sqrt{\beta_k^2 + \omega_k^2 + 2\beta_k\omega_k - 4\omega_k\beta_k + 4\Theta^2} \tag{5.2.22}$$

The equation is reduced to

$$= \frac{\beta_k + \omega_k}{2} \pm \frac{1}{2}\sqrt{\beta_k^2 + \omega_k^2 + 4\Theta^2 - 2\beta_k\omega_k} \tag{5.2.23}$$

The difference arise from the fact that the exciton energy is very much larger than the magnon energy [60], As a result, $\omega_k^2 - 2\beta_k\omega_k \ll \beta_k^2 + 4\Theta^2$.

The Eq. (5.2.23) reduced to

$$\varepsilon_k = \frac{1}{2}\left(\beta_k + \omega_k \pm \sqrt{\beta_k^2 + 4\Theta^2}\right) \tag{5.2.24}$$

let simplify equation under square root, by taking $(\beta_k + 2\Theta)^2 = \beta_k^2 + 4\Theta^2 + 4\beta_k\Theta$ however, $\beta_k\Theta \ll 1$ because, for example in GaAs, β_k=1.6x10^{-22}J [61] and $\beta_k \gg \Theta$ [57] thus, $(\beta_k + 2\Theta)^2 \cong \beta_k^2 + 4\Theta^2$, the Eq.(5.2.24) becomes

$$\varepsilon_k \cong \frac{1}{2}\left(\beta_k + \omega_k \pm \sqrt{(\beta_k + 2\Theta)^2}\right) \tag{5.2.25}$$

$$= \frac{1}{2}(\beta_k + \omega_k \pm (\beta_k + 2\Theta)) \tag{5.2.26}$$

In this case, we are interested in free magnon and magnon-exciton interaction

$$\varepsilon_k = \frac{1}{2}\omega_k - \Theta \tag{5.2.27}$$

$$\varepsilon_k \cong \eta k^2 - \Theta \tag{5.2.28}$$

where $\eta = \frac{1}{3} J x_m S z a^2$. From the Fig. 5.1, the graph of magnon dispersion energy in the the presence of interaction between the exciton and magnon is below the graph without coupling energy. From this we can deduce that the coupling energy decreases the magnon

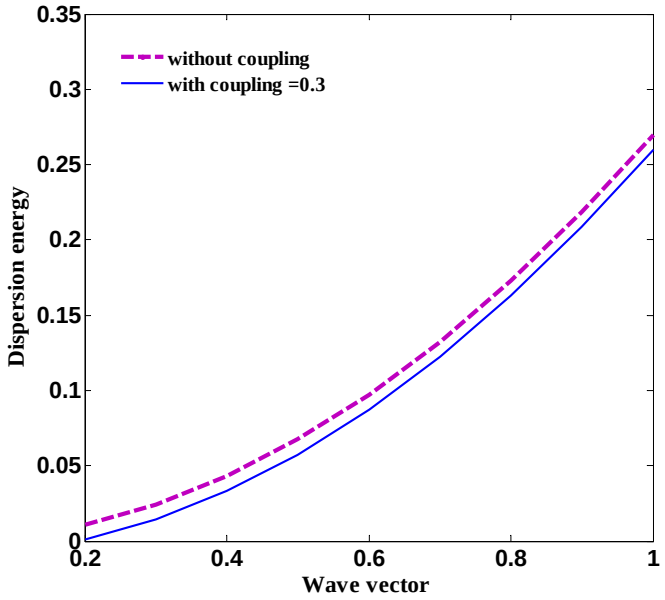

Figure 5.1: Shows variation of magnon dispersion energy with and without the coupling constant of magnon-exciton interaction.

dispersion energy.

5.2.1 Number of Magnons

To calculate the number of magnons excited at temperature T, the only other equation we shall require from Green functions theory is that defining the relationship between $\langle\langle A(t); B(t')\rangle\rangle_E$ which is the the energy (E) dependent Fourier transformation of Green function involving operators A(t) and B(t') and correlated function $< A(t)B(t') >$ for t=t' [62]. This may written as

$$\langle A(t)B(t')\rangle = i\int_{-\infty}^{\infty}\left(\frac{\langle\langle A(t); B(t')\rangle\rangle_{E+i\epsilon} - \langle\langle A(t); B(t')\rangle\rangle_{E-i\epsilon}}{e^{\beta E}-1}\right)e^{-iE(t-t')}dE \tag{5.2.29}$$

When the Eq.5.2.29 expressed by creation and annihilation operators of magnon, since $\langle ... \rangle$ refers to the quantum statistical average, it represents the average number of magnons

excited at temperature T which is denoted by $\langle b_k b_k^+ \rangle = \langle n_k \rangle$

$$< b_k b_k^+ >= i \int_{-\infty}^{\infty} \left(\frac{\langle\langle b_k; b_k^+ \rangle\rangle_{E+i\epsilon} - \langle\langle b_k; b_k^+ \rangle\rangle_{E-i\epsilon}}{e^{\beta E} - 1} \right) e^{-iE(t-t')} dE \tag{5.2.30}$$

where, E is the real energy of Green function that have at pole and ϵ is imaginary part of energy in complex plane [63].

Using the Dirac identity,

$$\frac{1}{x \pm i\epsilon} = P\frac{1}{x} \mp i\pi\delta(x) \tag{5.2.31}$$

$$\langle\langle b_k; b_k^+ \rangle\rangle_{E+i\epsilon} = \frac{1}{2\pi[(E + i\epsilon) - \epsilon_k]} \tag{5.2.32}$$

$$\langle\langle b_k; b_k^+ \rangle\rangle_{E+i\epsilon} = \frac{1}{2\pi}\left[\frac{P}{E - \varepsilon_k} - i\pi\delta(E - \varepsilon_k)\right] \tag{5.2.33}$$

Similarly,

$$\langle\langle b_k; b_k^+ \rangle\rangle_{E-i\epsilon} = \frac{1}{2\pi[(E - i\epsilon) - \varepsilon_k]} \tag{5.2.34}$$

$$= \frac{1}{2\pi}\left[\frac{P}{E - \varepsilon_k} + i\pi\delta(E - \varepsilon_k)\right] \tag{5.2.35}$$

where P is the principal part of the integral which exclude the poles. We want to treat singularity by shifting poles upward $(+i\epsilon)$ and downward $(i\epsilon)$ and $\pm\, of\ (i\pi\delta(\mathrm{x}))$ show the motion of particle counterclockwise (+) and clockwise (-) directions.

By substituting Eq. (5.2.33) and Eq. (5.2.35) in to Eq.(5.2.30) and at equal time correlation t=t', we get

$$< b_k b_k^+ >= i \int_{-\infty}^{\infty} \frac{\frac{1}{2\pi}\left[\frac{P}{E-\varepsilon_k} - i\pi\delta(E - \varepsilon_k)\right] - \left(\frac{1}{2\pi}\left[\frac{P}{E-\varepsilon_k} + i\pi\delta(E - \varepsilon_k)\right]\right)}{e^{\beta E} - 1} dE \tag{5.2.36}$$

$$= \frac{i}{2\pi} \frac{\int_{-\infty}^{\infty}[-i\pi\delta(E - \epsilon_k) - i\pi\delta(E - \epsilon_k]}{e^{\beta E} - 1} dE \tag{5.2.37}$$

$$= \frac{i}{2\pi} \frac{\int_{-\infty}^{\infty}[-2i\pi\delta(E - \epsilon_k)]}{e^{\beta E} - 1} dE \tag{5.2.38}$$

$$= i \int_{-\infty}^{\infty} -i \frac{\delta(E - \varepsilon_k)}{e^{\beta E} - 1} dE \tag{5.2.39}$$

$$\langle b_k b_k^+ langle = \int_{-\infty}^{\infty} \frac{\delta(E - \varepsilon_k)}{e^{\beta E} - 1} dE \tag{5.2.40}$$

At $E = \varepsilon_k$, $\delta(E - \varepsilon_k)$=1 and otherwise zero, hence for a single mode

$$\langle b_k b_k^+ \rangle = \frac{1}{e^{\beta \varepsilon_k} - 1} \tag{5.2.41}$$

where $\beta = \frac{1}{K_B T}$ and $\langle b_k b_k^+ \rangle = \langle n_k \rangle$. Therefore,

$$\langle n_k \rangle = \frac{1}{e^{\beta \varepsilon_k} - 1} \tag{5.2.42}$$

this show that

$$\epsilon_k = \frac{1}{\beta} \ln \left[\frac{1}{\langle n_k \rangle} + 1 \right] \tag{5.2.43}$$

indicating dispersion and number of magnon have a logarithmic relationship, and so is for the total number of magnons.

When Eq. (5.2.28) is substituted in to Eq. (5.2.41)

$$\langle b_k b_k^+ \rangle = \frac{1}{e^{\beta(\eta k^2 - \Theta)} - 1} \tag{5.2.44}$$

The mean number of magnons with wave vector k at temperature T will be

$$\langle n_k \rangle = \frac{1}{e^{\beta(\eta k^2 - \Theta)} - 1} \tag{5.2.45}$$

The equation shows that the magnon number in a single mode is also affected by magnon-exciton coupling constant. The total number of excited magnons in all modes at temperature T will be

$$\sum_k \langle n_k \rangle = \sum_k \langle b_k b_k^+ \rangle = \sum_k \frac{1}{e^{\beta(\eta k^2 - \Theta)} - 1} \tag{5.2.46}$$

Let estimate the integral on Eq. (5.2.46) which is total number of magnons excited at temperature T, this need surface integral.

$$\sum_k \langle n_k \rangle = \frac{1}{2\pi^2} \int_0^{\infty} \frac{k^2}{e^{\beta(\eta k^2 - \Theta)} - 1} dk \tag{5.2.47}$$

Let, $x{=}\beta\eta k^2 - \beta\Theta$, $dx = 2\beta\eta k\ dk$ and $k^2 = \frac{x+\beta\Theta}{\beta\eta}$ also dk = $\frac{dx}{2(\beta\eta)^{1/2}(x+\beta\Theta)^{1/2}}$

$$\sum_k \langle n_k \rangle = \frac{1}{2\pi^2} \int_{-\beta\Theta}^{\infty} \frac{\frac{x+\beta\Theta}{\beta\eta}\ \frac{dx}{2(\beta\eta)^{1/2}(x+\beta\Theta)^{1/2}}}{e^x - 1} \tag{5.2.48}$$

$$\sum_k \langle n_k \rangle = \left(\frac{1}{2\pi^2}\right) \frac{1}{2(\beta\eta)^{3/2}} \int_{-\beta\Theta}^{\infty} \frac{(x+\beta\Theta)^{1/2}}{e^x - 1} dx \tag{5.2.49}$$

This can be expressed as

$$\sum_k \langle n_k \rangle = \frac{1}{2\pi^2} \left[\frac{1}{2(\beta\eta)^{3/2}} \int_{-\beta\Theta}^{0} \frac{(x+\beta\Theta)^{1/2}}{e^x - 1} dx + \frac{1}{2(\beta\eta)^{3/2}} \int_{0}^{\infty} \frac{(x+\beta\Theta)^{1/2}}{e^x - 1} dx \right] \tag{5.2.50}$$

The first term has least contribution to our objective, so work with

$$\sum_k \langle n_k \rangle = \frac{1}{2\pi^2} \left[\frac{1}{2(\beta\eta)^{3/2}} \int_{0}^{\infty} \frac{(x+\beta\Theta)^{1/2}}{e^x - 1} dx \right] \tag{5.2.51}$$

Let expand the numerator under square root $(x+\beta\Theta)^{1/2}$, where $\beta\Theta$is very small

$$f(x+\beta\Theta) = f(0) + f^{'}(0)\beta\Theta + \frac{f^{''}(0)(\beta\Theta)^2}{2!} + \frac{f^{'''}(0)(\beta\Theta)^3}{3!} + \frac{f^{''''}(0)(\beta\Theta)^4}{4!} + ... \tag{5.2.52}$$

$$f(x+\beta\Theta) = f(x) + f^{'}(x)\beta\Theta + \frac{1}{2!}f^{''}(x)(\beta\Theta)^2 + \frac{1}{3!}f^{'''}(x)(\beta\Theta)^3 + \frac{1}{4!}f^{''''}(x)(\beta\Theta)^4 + ... \tag{5.2.53}$$

$$f(x+\beta\Theta)^{1/2} = x^{1/2} + \frac{1}{2}x^{-1/2}(\beta\Theta) - \frac{1}{8}x^{-3/2}(\beta\Theta)^2 - \frac{1}{16}x^{-5/2}(\beta\Theta)^3 + ... \tag{5.2.54}$$

The last two terms are very much small numbers, let take the first two

$$f(x+\beta\Theta)^{1/2} = x^{1/2} + \frac{1}{2}x^{-1/2}\beta\Theta \tag{5.2.55}$$

$$\sum_k \langle n_k \rangle = \frac{1}{4\pi^2} \left[\frac{1}{(\beta\eta)^{3/2}} \int_{0}^{\infty} \frac{x^{1/2} + \frac{1}{2}x^{-1/2}\beta\Theta}{e^x - 1} dx \right] \tag{5.2.56}$$

$$\sum_k \langle n_k \rangle = \frac{1}{4\pi^2} \left[\frac{1}{(\beta\eta)^{3/2}} \int_{0}^{\infty} \frac{x^{1/2}}{e^x - 1} dx + \frac{\beta\Theta}{(\beta\eta)^{3/2}} \int_{0}^{\infty} \frac{1}{2} \frac{x^{-1/2}}{e^x - 1} dx \right] \tag{5.2.57}$$

We can evaluating by expanding integral in series: since $e^{-x} \leq 1$

$$\frac{x^{1/2}}{e^x - 1} = e^{-x}x^{1/2}(1 + e^{-x} + e^{-2x} + e^{-3x} + ...) = \sum_{n-1}^{\infty} e^{-nx}x^{1/2} \tag{5.2.58}$$

so, $\int_0^\infty \frac{x^{1/2}}{e^x-1}dx = \sum_{n-1}^\infty \int_0^\infty e^{-nx}x^{1/2}dx = 1/2! \sum_{n=1}^\infty \frac{1}{n^{1/2+1}} = 0.886 \sum_{n=1}^\infty \frac{1}{n^{3/2}}$ $\sum_{n=1}^\infty \frac{1}{n^{3/2}} = \frac{1}{1^{3/2}} + \frac{1}{2^{3/2}} + \frac{1}{3^{3/2}} + \frac{1}{4^{3/2}} + ...$

We use inequalities to get a quick estimate of this series that would be too tedious to sum itself.

$\sum_{n=1}^\infty \frac{1}{n^{3/2}} = 1 + \frac{1}{2^{3/2}} + \frac{1}{3^{3/2}} + \sum_4^\infty \frac{1}{n^{3/2}}$

The last sum lies between two integrals which are upper and lower bounds.

$\int_3^\infty \frac{1}{x^{3/2}}dx > \sum_4^\infty \frac{1}{n^{3/2}} > \int_4^\infty \frac{1}{x^{3/2}}dx$

That is between 1.1547 and 1. Now we will estimate the whole sum by adding the first three terms explicitly and taking the arithmetic average of these two bounds

$\sum_{n=1}^\infty \frac{1}{n^{3/2}} = 1 + \frac{1}{2^{3/2}} + \frac{1}{3^{3/2}} + \frac{1}{2}(1.1547 + 1) = 2.623$

$$\int_0^\infty \frac{x^{1/2}}{e^x - 1}dx = \sum_{n-1}^\infty e^{-nx}x^{1/2}dx = 0.886 \sum_{n=1}^\infty \frac{1}{n^{3/2}} \approx 2.3239 \tag{5.2.59}$$

and similarly, $\frac{1}{2}\int_0^\infty \frac{x^{-1/2}}{e^x-1}dx \approx 1771.15$.

The Eq. (5.2.57) becomes

$$\sum_k \langle n_k \rangle = \frac{1}{4\pi^2}\left[\frac{1}{(\beta\eta)^{3/2}}(2.3239) + \frac{\beta\Theta}{(\beta\eta)^{3/2}}(3542.3)\right] \tag{5.2.60}$$

$$\sum_k \langle n_k \rangle = 0.0589\frac{(k_BT)^{3/2}}{(Jx_mza^2S)^{3/2}} + 44.91\frac{(K_BT)^{1/2}\Theta}{(Jx_mza^2S)^{3/2}} \tag{5.2.61}$$

$0.0589\frac{(K_B)^{3/2}}{(JS)^{3/2}} = \lambda \; and \; 44.91\frac{(K_B)^{1/2}}{(JS)^{3/2}} = \nu$ are obtained based on standard values of constants in the expression.

$$\sum_k \langle n_k \rangle = \frac{\lambda T^{3/2}}{(x_mz)^{3/2}a^3} + \frac{\nu\Theta T^{1/2}}{(x_mz)^{3/2}a^3} \tag{5.2.62}$$

$$\sum_k \langle n_k \rangle = \frac{1}{(x_mz)^{3/2}a^3}\left[\lambda T^{3/2} + \nu\Theta T^{1/2}\right] \tag{5.2.63}$$

From Eq. (5.2.63), we can plot total number of magnons versus temperature. For better estimation of the exchange interaction of local magnetic moments at different sites separated by distance of GaAs lattice constant ($a = 5.56A^0$), $J = 31.195 \times 10^{-23}$Joules, spin of the Mn 3d sub-shell of an atom S = 5/2, $x_m = 0.053$ and the Boltzmann constant $k_B = 1.38 \times 10^{-23}J/K$ are used [35]. On Fig. 5.2 (**a**) total number of magnons

can be affected by the coupling constant Θ. It indicated that, like temperature, the magnon-exciton coupling energy increases the total number of magnon. This is because, magnon-exciton coupling is an interaction arising out of the coupling between a pair of nearest-neighbor ions where one of the ions is raised to an excited electronic state and has its spin component changed by unity, while the other ion has an accompanying unit change in spin to conserve total spin of the system [57]. The red curve in Fig. 5.2 (**b**) refers to the behavior of number of magnons at temperature greater than one in the absence of coupling constat. Number of magnon and temperature has $T^{3/2}$ relationship, because of $T^{3/2}$ is more pronounced than $T^{1/2}$ for $T > 1K$. Generally, we can infer that the coupling constant decreases the magnetization by increasing the number of magnons at the same time enhancing the scattering of localized magnetic spins.

5.2.2 Magnetization

Temperature dependence of the magnetization of a ferromagnetic material at low temperature was explained by F. Bloch who originally introduced the concept of spin wave [48].

$$M(T) = M(0) - g\mu_B \sum_k \langle n_k \rangle \tag{5.2.64}$$

Where$M(0) = g\mu_B nS$ is ground state magnetization at absolute zero temperature where all spins are parallel.

$$M(T) = g\mu_B nS\left(1 - \frac{1}{nS}\sum_k \langle n_k \rangle\right) \tag{5.2.65}$$

Substituting Eq. (5.2.63) into Eq. (5.2.65)

$$M(T) = g\mu_B nS\left[1 - \frac{1}{4S(x_m z)^{3/2} n a^3}\left(\lambda T^{3/2} + \nu\Theta T^{1/2}\right)\right] \tag{5.2.66}$$

where n is number of atoms per unit volume of lattice cell ($n = \frac{N}{V} = \frac{N}{a^3}$) and N is 1, 2, 4 for Sc, bcc and fcc lattice respectively [6]. For instance, for (Ga,Mn)As has fcc lattice structure with n= $\frac{4}{a^3}$. The ratio of temperature dependent magnetization M(T) and zero the temperature magnetization M(0) gives

$$\frac{M(T)}{M(0)} = 1 - \frac{1}{4S(x_m z)^{3/2}}\left(\lambda T^{3/2} + \nu\Theta T^{1/2}\right) \tag{5.2.67}$$

When $\frac{M(T)}{M(0)}$ approaches to zero, the temperature T approaches to transition temperature (T_c) of ferromagnetic, which shows the excitation of thermal magnons leads to the decrease of magnetization with increasing temperature until it falls to zero at curie temperature where the material becomes paramagnetic [38]. The mean field theory does not give good explanation of the variation of magnetization at low temperatures. The mean field theory predicts exponentially convergence of the magnetization to the value at zero temperature [26]. From Eq. (5.2.67) and Fig. 5.3 (**a**), the reduced magnetization at low temperature $T < 1K$ is less depend on $T^{3/2}$ which agreed with [64] but, more depend on $T^{1/2}$ including coupling constant which accelerate the decreasing in magnetization due to increasing in temperatures. In Fig. 5.3 (**b**) the fraction of magnetization at $T > 1K$ is depend on $T^{3/2}$ in the absence of coupling constant. We see that the saturation magnetization decreases with increasing temperature until it falls to zero at the curie temperature. Depend on the limiting case of $\frac{M(T)}{M(0)}$, the concentration of the magnetic impurity x_m, is linearly related to the ferromagnetic transition temperature T_c.

$$0 = 1 - \frac{1}{4S(x_m z)^{3/2}}\left(\lambda T_c^{3/2} + \nu\Theta T_c^{1/2}\right)$$

$$1 = \frac{1}{4S(x_m z)^{3/2}}\left(\lambda T_c^{3/2} + \nu\Theta T_c^{1/2}\right)$$

$$x_m = \frac{1}{(4S)^{2/3} z}\left(\lambda T_c^{3/2} + \nu\Theta T_c^{1/2}\right)^{2/3} \tag{5.2.68}$$

Fig. 5.4(**a**) shows the direct proportionality relation between Curie temperature T_c and impurity concentration x_m as given by Ohino who proposed the relation as $T_c \cong 2000x_m \pm 10k$ for $x_m < 0.05$ [39]. But, Fig. 5.4 (**b**), show that the $T_c \cong 2000x_m \pm 10k$ relation does not work for lower values of Curie temperature ($T_c < 1K$) limit. From Fig. 5.4 (**b**), initially, we can see $T_c = 0$, for both figures with and without coupling constant even though the impurity concentration x_m is increasing. This shows that there is no direct proportionality between impurity x_m and Curie temperature T_c for lower temperatures. Then, the graph with coupling constant observed below the graph of without coupling energy. This indicated that the magnon-exciton interaction decreases Curie temperature by enhancing disorder of spins and so is for $T_c > 1K$.

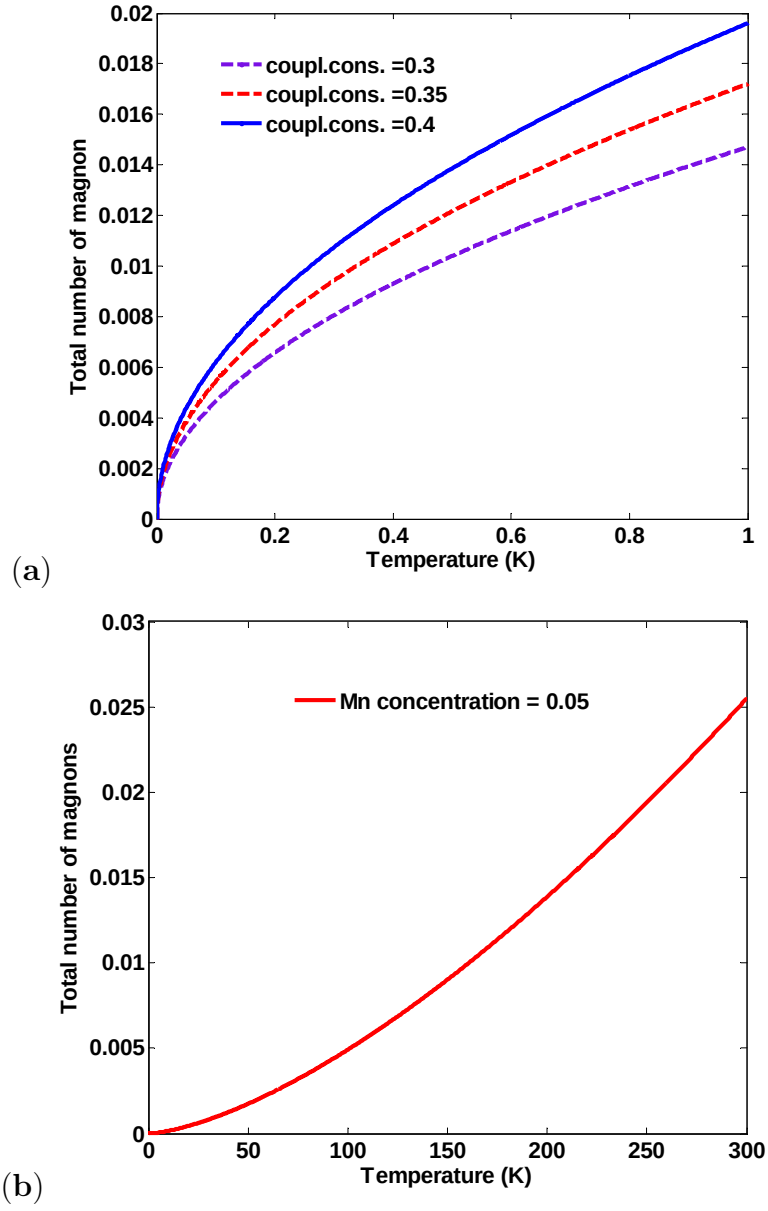

Figure 5.2: Number of magnon versus temperature less than one with coupling constant Θ =0.3, 0.35 and 0.4 (**a**) and greater than one without coupling constant (**b**) .

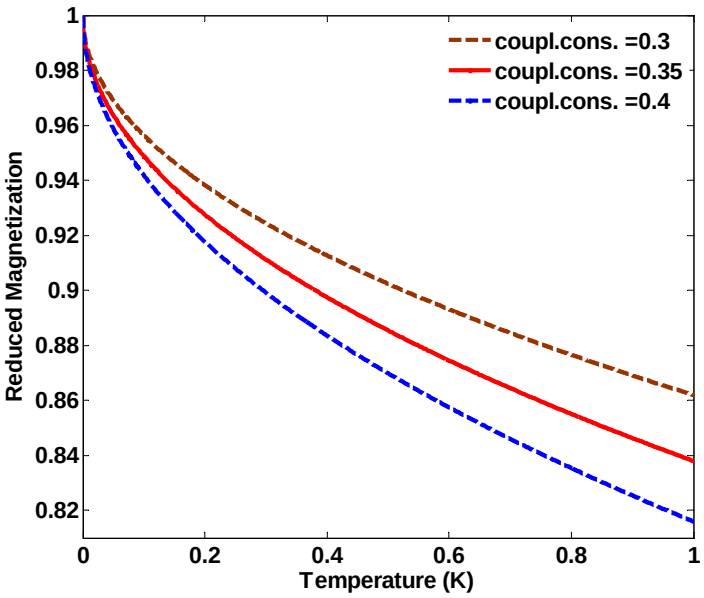

(**a**)

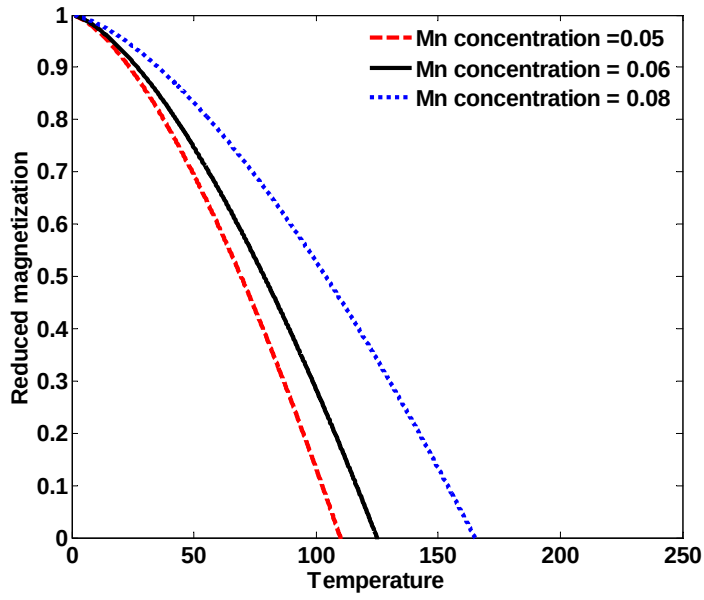

(**b**)

Figure 5.3: Reduced magnetization versus temperature with coupling (**a**) and for $x_m = 0.05$, $x_m = 0.06$ and $x_m = 0.08$ without coupling (**b**).

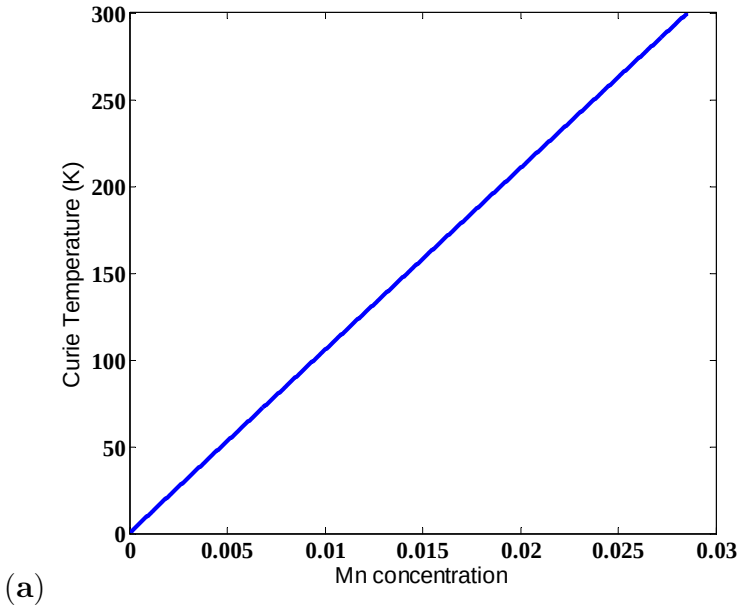

(a)

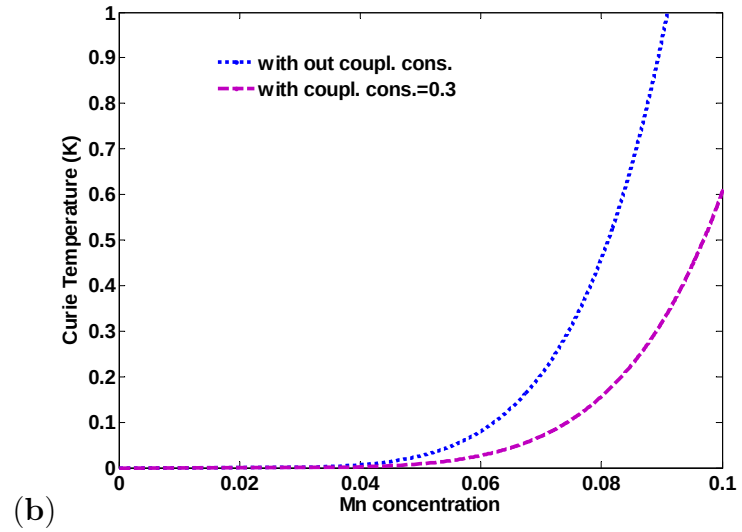

(b)

Figure 5.4: (a) A linear dependance of T_c with magnetic concentration for higher temperature ($T_c > 1K$). (b) Plot of T_c versus x_m for lower temperature ($T_c < 1K$).

Chapter 6

Summary And Conclusion

Diluted magnetic semiconductors (DMS) have both semiconducting and magnetic properties which provide the possibility to manipulate electron charge and spin at the same time and opens a new field in semiconductor technology. In conventional electronic devices, information is stored and transmitted by the flow of electricity in the form of negatively charged subatomic particle called electron. In spintronics, however, information is stored and transmitted using additional degrees of freedom of electrons which act like compass needle pointing either up or down.

DMSs are known by their special property, like addition of magnetic impurities instead of few portions of compound semiconductors at cation site at most. These magnetic ions provide a localized spins and act as an accepter in most III-V semiconductors so that it can also provide holes and carrier-mediated ferromagnetism. In this case T_c is understood as to vary with density of Mn ions and holes. The ground state has no magnons, i.e., $\langle n_k \rangle = 0$ at zero temperature. The ground state energy is therefore simply interaction energy of all spins pointing in the same direction with maximum value of S along z direction. As temperature increases, number of excited magnons also increase being thermally agitated. Therefore, spin waves make $\langle S_j^z \rangle$ less than the maximum value of S, decrease magnetization and make weak ferromagnetic order of the system. In reduced magnetization $\left[\frac{M(T)}{M(0)}\right]$ versus temperature graph, $\frac{M(T)}{M(0)}$ is decreasing with increasing temperature. Below T_c there is saturation magnetization and above T_c there is a paramagnetic region.

The main obstacle for application of DMSs in spintronics technology is the low value of Curie temperature T_c. Therefore, if T_c of the DMSs can be increased, there will be a possibility of utilizing the system under consideration for spintronics purpose at room

temperature. To circumvent such limitations effects of visible and non-visible factors have been studied. One of these is effect magnon-exciton interaction which we discussed in this work. Our investigation indicated that ferromagnetic transition temperature T_c varies with the impurity constatation x_m in DMSs and the two parameters have direct proportionality at higher temperatures and less affected by the coupling parameter. But for temperatures less than one, the direct proportionality is violated with dominating magnon-exciton interaction energy. Hence, the coupling energy of magnon and exciton decreases curie temperature T_c for both higher and lower temperature values enhancing total number of magnons.

Bibliography

[1] S. M. SZE. M. K. LEE (2010). *Semiconductor devices physics and Technology*, 3^{rd} ed., John Wiley and Sons. Inc.

[2] T. Dietl, A. Haury and Y. Merle, phys. Rev. **B55**, R3347 (1997).

[3] M. dos Sato (2013). *Magnetic and Magnetic interaction*, F. Julich, Germany.

[4] S. Cho, G. B. Cha, S.C. Hong, Y. Kim, Y. J. Zhao, A. J. Freemann, J. B Ketterson, B. J. Kim, Y. C. Kim, B. C. Cho, Phys. Rev. Lett., **88**, 257203 (2002).

[5] G. A. Medvedkin, T. Ishibashi, T. Nishi, K. Hiyata, J. Appl. phys.**39**, 949 (2000).

[6] S. Das Sarma, Phys. Rev. A**64**, 042312 (2001).

[7] K. Khazen (2008). Phd. Desseration in *Ferromagnetic reason once Investigation of GaMnAs Nanometric layers*.

[8] J. Collet, J. Phys. Chem. Sol. **46**, NO. 4, 422 (1985).

[9] B. G. Yacob (2004). *Semiconductor materials: An introduction to basic principles*, first ed., Kuluwer Acadamic publisher, New York.

[10] J. P. Colinge and C.A. Colinge, (1997). *Physics of semiconductor devices*, Kluwer Acadamic publishare, New York.

[11] S. Bremner (2009). *Solar Electric system*, University of Delaware.

[12] F. C. Chang, K. C. Shen, H. M. Chung, M. C. Lee,W. H. Chen and W. K. Chen, J. Phys. **40**, No. 6 (2002)

[13] C. Kittle (2005). *Introduction to solid state physic*, 8^{th} ed., Jhon Wiley and Son Inc.

[14] A. Kastalky, S. Luury and B. Spivak, semiconductor high energy radiations intillation de tector. Email: serge:Lury@ stony Brook. edc.

[15] A. Owen, A.Peacok, Physics research **A531**, 37 (2004).

[16] D. M. Chapin, C. S. Fuller and G. L. Pearson **25**, 677 (1954).

[17] H.Hayashi, (2011). *Development of semiconductor devices-in search of Immense possibility*, world scientific publishing campany.

[18] S. J. Ward, (1995). *Compound semiconductor device physic*, 3^{rd} ed., Walther Meibner institut.

[19] L. M. Sandratskii and P. Bruno, Lect. Notes phys.**3-130**, 678 (2005).

[20] H. Hermann, S. Bennett, L. Menon, J. Appl. Phys. **104**, 024309 (2008)

[21] N. W. Ashkroft N. David Mermin, (2001). *Solid state physics*, 1^{st} print, sounder college publishing, India.

[22] E. Y. Tsymbal, phys. **927**, 3 (2002)

[23] J. A Gaj, J. Kossut, Spring series in mat. sci. **144**, 1007 (2010).

[24] http// WWW2. physics . ox.ac.uk/ student/ cource- materials/c3- condenced-major option, Hilary (2013)

[25] C. M. Julien. A. Ait-Salab. A. Mauger, F. Gendron, Ionics **12**, 32 (2006).

[26] D. Giri, M.Panday, Int. J. Adv. Comp. Tech.**4**, 2319 (2005).

[27] T. Hayashi, Y. Hashimoto, S. Katsumto and Y. Iye Appl. Phys. Lett. **78**, No. 12 (2001)..

[28] M. H. Kane, (2007). A Phd desseration, *Investigation of the stablity of wide band gap Diluted magnetic semiconductors for Spintronics.*

[29] H. Ohno, science **281**, 951 (1998).

[30] G. Prinz, J. Mag. Mag. mat., **200**, 58 (1999)

[31] T. Dietl, Phys. Lett.**46**, 02668 (2003).

[32] J. Mahanty, (1974). *The Green function methode in Solid State Physics*, East-West Press, New Delhi.)

[33] R. Rajaram, (2007). *Study of magnetism in diluted magnetic semiconductor based on III-V Nitrates*, (unpublished).

[34] N. Zheng, (2008), *Introduction to Diluted Magnetic Semiconductors*, The University of Tennessee, (unpublished).

[35] T. Heinzel, (2007). *Mesoscopic Electronics in Solid State Nanostructure*, 2^{nd} ed., Wiley-Vch and Co.Kga.

[36] K. Sato, T. Ishi bashi, K. Minami, H. Yuasa, J. Jogo, T. Nagatsuka, A. Mizusawa, Y. Kangawa a and A. Koukitu J. of physics and chemistry of solid **66**, 2030 (2005).

[37] D. E. Nikonov, M. Hill, G Bourianoff, J. Phys. A**1**,01455502 (2007)

[38] H. Ohno, T. Dieti, F. Matsukura, phys. Rev. **B63**, 195205 (2001).

[39] A. Sahele, (2011), (MSc thesis, Addis Ababa University), *Study of critical temperature of Diluted magnetic semiconductors (Ga,Mn)As.*

[40] C. Amante, K. Dharamvir, J. Mod. Phys. **4**, 1563 (2013).

[41] Z. Wilamowski and A. M. Werpachowska, Mat. sci. **24,** 3, (2006).

[42] H. Ohno, A. Shen, F. Matsukura, and et al , app. phys. lett. **69**, 363 (1996)

[43] S. J. Pearton, C. R Abernathy, D. P. Nortton, A. F. Hebard, Y. D. Park, L. A. Boatnel and J. D. Budia, R **40**, 137 (2003).

[44] Y. Solomon, (2010), (MSc thesis, Addis Ababa University), *The study of Ferromagnetic and Antiferromagnetism in DMS GaMAs*, MSc. thesis.

[45] Z. Wilamowski and A. M. Werpa chowska, Mat. Sci. **24**, (2006)

[46] M. C. Prestgard, G. P. Siegel and A. Tiwari, Adv. Matt. Lett.**5**, 247 (2013).

[47] M. Linnarsson, Phys. Rev. **B55**, 6935 (1997).

[48] W. Schweika, S. V. Maleyev, TH. Bruckel, V. P. Plalchty and L. P. Regnauet Euro. Phys. Lett. **60**, 452 (2002).

[49] T. Nie, J. Tang, K. L. Wang, J. Cr. Growth **10**, 1016 (2015).

[50] A. Fert and I. A. Campbell, J. Phys. F**6**, 849 (1976).

[51] S. Balmukund Rahi and P. Rastogi, Int. J. Adv. in Eng. and Tech. **6**, 696 (2013)

[52] J. B. Parkinson, J. Appl. Phys. **40**, 1 (1969).

[53] J. Fabian and S. Das Sarma, Rev. Mod. Phys. **76**,323 (2004).

[54] Y. V. Pershin, Cond-mat/0311223, www. arXiv.org.

[55] A. P. Crackinell, Mag. Cr. Mat. **33**, 174 (1975).

[56] D. D. Richardson, J. Phys. **27**, 457 (1974).

[57] V K. Thai and H. A. Proc. Natl. Conf. Theor. **36**, 107 (2011).

[58] C. Amente and P. Singh, Modern Phys. Lett. B **25**, 280 (2010).

[59] A. P. Crackinell, Mag. Cr. Mat. **33**, 174 (1975).

[60] Y. sido, (2007). *Theorotical study of excitons in semiconductor quantum wires and related systems.*

[61] J. D. Patterson, (2010). *Solid state physics: Introduction to Theory*, 2nd, ed., A. Wesley publishing campany Germany.

[62] M. Nolting, (2009). *Fundamentals of many body physics*, Verlag Berlin Heidelberg.

[63] N. Ba An and L. T. Tuong, Solid state comun. **80**, 479 (1991).

[64] Xun xu, S. Windodo and M. Fujii, Conf. Series **400**, 032112 (2012).

DECLARATION

I hereby declare that this MSc is my original work and has not been presented for a degree in any other universities, and that all sources of material used for the dissertation have been duly acknowledged.

Name: Dereje Fufa

Signature: _____

This MSc has been submitted to for examination with my approval as university advisor.

Name: Dr. Chernet Amente
Signature: _____

Place and date of submission:

Department of Physics
Addis Ababa University
August 11, 2017